

# Technical University of Dortmund

Master of Science in Manufacturing Technology (MMT)

Faculty of Mechanical Engineering

Chair for Reliability Engineering

Submitted to: Univ-Prof. Dr. Matthias Faes

## **Project work:**

# **Effects of lubricants in the force signal, tool wear and workpiece quality in blanking manufacturing process.**

Sommer semester 2023

Submitted by:

**Gabriel Jimenez (229675)**

Submission date: July, 13<sup>th</sup> 2023

## Contents

Contents .....	II
List of tables .....	III
List of figures .....	IV
1. Introduction .....	1
1.1. Research objectives .....	1
2. Theoretical background .....	3
2.1. Blanking manufacturing process .....	3
2.2. Fast Fourier transform .....	7
2.3. Power spectrum analysis .....	8
2.4. Blanking manufacturing machine:.....	8
2.5. Profilometer.....	9
3. Literature review. ....	10
3.1. Machine learning .....	10
3.1.1. Gaussian process regression (GPR).....	11
4. Problem definition .....	12
4.1. Methodology and experiment details .....	12
5. Experimental results .....	23
5.1. Force signal .....	23
5.2. Impulse evolution .....	31
5.3. Tool wear.....	34
5.3.1. Edge radius wear evolution .....	34
5.3.2. Roughness depth Rz evolution at punch surfaces.....	35
5.4. Workpiece quality .....	38
5.4.1. Shear zone roughness evolution .....	38
5.4.2. Cross section evolution.....	40
5.5. Ranking and comparison .....	41
6. Future experimental considerations .....	42
7. Conclusions .....	44
8. Bibliography .....	46
9. Appendix .....	49
9.1. Appendix A .....	49
9.2. Appendix B.....	50
9.3. Appendix C.....	52

## List of tables

<b>Table 3-1</b> Mechanical properties .....	13
<b>Table 3-2</b> Experiments designations .....	13
<b>Table 3-3</b> Measuring parameters .....	15
<b>Table 3-4</b> Ponderation Values .....	22
<b>Table 3-5</b> Grading criteria .....	22
<b>Table 4-1</b> FFT frequency intervals .....	25
<b>Table 4-2</b> PSD evolution. GPR and linear fitting results and comparison .....	29
<b>Table 4-3</b> Total power results and comparison .....	30
<b>Table 4-4</b> Impulse evolution. GPR and linear fitting results and comparison .....	32
<b>Table 4-5</b> Total impulse results and comparison.....	33
<b>Table 4-6</b> Edge radius measurements.....	34
<b>Table 4-7</b> Edge radius. GPR and linear fitting results and comparison .....	35
<b>Table 4-8</b> Roughness depth Rz evolution.....	36
<b>Table 4-9</b> Roughness evolution. GPR and linear fitting results and comparison.....	37
<b>Table 4-10</b> Average shear zone sample roughness.....	38
<b>Table 4-11</b> Shear zone roughness evolution. GPR and linear fitting results and comparison.....	39
<b>Table 4-12</b> Ponderation and grading results.....	41
<b>Table 8-1</b> Punch 1. Cross section zones evolution data .....	52
<b>Table 8-2</b> Punch 2. Cross section zones evolution data .....	53
<b>Table 8-3</b> Punch 3. Cross section zones evolution data .....	54
<b>Table 8-4</b> Punch 4. Cross section zones evolution data .....	55

## List of figures

<b>Figure 2-1</b> Blanking and Piercing schematic representation.....	3
<b>Figure 2-2</b> Phases of the blanking process. [1] .....	3
<b>Figure 2-3</b> Force-time curve during the shearing process [3] .....	4
<b>Figure 2-4</b> Cutting tool edges [3] .....	5
<b>Figure 2-5</b> Different zones if the barked workpiece cross section [2].....	5
<b>Figure 2-6</b> Fine blanking and normal shearing comparison [2] .....	7
<b>Figure 2-7</b> Signal decomposition representation in the time and frequency domain. [6] .....	8
<b>Figure 2-8</b> TruPunch 5000 blanking machine. [8] .....	9
<b>Figure 2-9</b> Keyence optical measuring machine .....	9
<b>Figure 4-1</b> Set and rows representation.....	12
<b>Figure 4-2</b> Square punch. ....	12
<b>Figure 3-3</b> Measuring points on the punching head for measuring the punching force.....	14
<b>Figure 3-4</b> Frequency and power analysis workflow .....	16
<b>Figure 3-5</b> Impulse calculation workflow .....	17
<b>Figure 3-6</b> Edge radii measurements, a) Punch at 45 degrees b) 3D surface representation, c) Measurement lines representation, d) Edge radius .....	18
<b>Figure 3-7</b> Comparison at the punch surface quality after a) 988 strokes and b) 24700 strokes for punch 1. ....	19
<b>Figure 3-8</b> Roughness measurements.....	19
<b>Figure 3-9</b> Roughness sample measurement. a) measurement length, b) 3D surface representation, c) roughness profile.....	20
<b>Figure 3-10</b> Sample cross-section .....	21
<b>Figure 3-11</b> Sample cross-section measurements. ....	21
<b>Figure 4-1</b> Force signal related to punch 1.....	23
<b>Figure 4-2</b> Single stroke. Force signal for punch.....	23
<b>Figure 4-3</b> FFT of a single stroke. Punch 1.....	24
<b>Figure 4-4</b> FFT evolution along each stroke .....	24
<b>Figure 4-5</b> FFT comparison of every experiment at the first stroke. ....	25
<b>Figure 4-6</b> Peak frequency intervals evolution .....	26
<b>Figure 4-7</b> PSD evolution along each stroke.....	27
<b>Figure 4-8</b> Power evolution of the force signal (Scatter plot).....	28
<b>Figure 4-9</b> Power evolution of the force signal (GPR tendency lines). ....	28
<b>Figure 4-10</b> Power evolution of the force signal (Linear fitting). ....	29
<b>Figure 4-11</b> Total power contained in every force signal. ....	30
<b>Figure 4-12</b> Impulse evolution of the force signal (Scatter plot) .....	31
<b>Figure 4-13</b> Impulse evolution of the force signal (GPR and linear fitting) .....	32
<b>Figure 4-14</b> Total impulse contained in every force signal.....	33
<b>Figure 4-15</b> Edge radius evolution.....	34
<b>Figure 4-16</b> Roughness evolution of the punch surfaces. (GPR and Linear regression) .....	37
<b>Figure 4-17</b> Roughness sample evolution (GPR and Linear regressions).....	39
<b>Figure 4-18</b> Sample cross-section evolution for every experiment.....	40

## 1. Introduction

The quality of a product in a manufacturing process has always been a key factor in production. The maintenance and the tools involved in the machine have a direct relationship on how the final product is conceived. In a blanking manufacturing process, the punch is the principal component affected by wear and abrasion due to the shear strength in the metal sheet. This creates severe tribological conditions highly prone to develop pick-up workpiece material at the punch surface which creates wear. The wear of the tool entails more maintenance for the machine involved, higher cost of production, lower quality of the product, increment of the post-processing processes and more energy consumption. Lubricants, on the other hand, could provide beneficial effects in the process, by reducing the friction and abrasion suffered by the punch.

To address these problems, it is important to study the tool wear evolution and how the quality of the workpiece develops in time, in order to properly address a good maintenance strategy and reduce the previous mentioned factors. Therefore, some experiments will be carried out with different types of lubrication and then compared in order to decide the proper selection of lubricant. To estimate and predict the behavior of tool wear and quality, a machine-learning method such a Gaussian Process Regression will be implemented in the data analysis.

### 1.1. Research objectives

The primary goal of this research is to study the influence of three different lubricants in the blanking manufacturing process and determine how they can relate to the force signal development, tool wear and quality evolution of the workpiece. Thus, four different experiments are going to be conducted, one without the effects of lubrications and three others with lubricants. The data acquired in the results will be analyzed with a machine-learning technique to estimate the different behaviors with regression modelling and compared so the best lubrication option can be selected for production. In order to implement machine-learning techniques in these different studies (tool wear, force signal analysis and quality evolution), the proper acquisition of the data should be taken into consideration. The following research topics will address the general objective:

- **Force signal:** The force signals will be collected and analyzed with a proper sample frequency so the accuracy and reliability of the machine learning numerical method can be applied, thus the evolution of the signal over time can be studied. The methods used to analyze the force signal will be:
  - Power spectral density (PSD): By means of the fast Fourier, transform (FFT) the PSD will provide the amount of energy contained in the signal.
  - Impulse (cutting work) evolution: By means of the integration of the force over time will provide the amount of work given at every stroke and the effects of the cutting tool in the process.
- **Tool wear evolution:** In order to study the tool wear for the blanking manufacturing process, the following studies will be carried out.
  - Edge radius wear evolution: In every cutting process, it is important to measure how sharp the tool is kept and the edge radius determines the sharpness. For every experiment, the

evolution of the edge radius along every stroke will be measured and thus the associated regression of these tendencies calculated.

- Roughness depth at punch surfaces: The cutting tool not only loses its sharpness but also different effects such as abrasion and adhesion could lead to tool wear at the surfaces which will affect not only the force signal but also the quality of the workpiece.
- **Workpiece quality**: is the key criteria in every manufacturing process and its evolution will provide a clear view on the effects of the lubricants in the final product. The most relevant factors to study within this project are the following:
  - Roughness evolution: It can determine how good the blanking process was performed and therefore the quality of the cut. A higher roughness at the shearing zone of the workpiece will result in additional post-processing methods and costs.
  - Cross section evolution: During the different experiments with and without lubrication, a number of samples will be collected to evaluate how each of the zones of the cross section evolves within the number of strokes.

Finally, after analyzing the results, the best lubricant from the experiments will be selected. The key criteria for the selection will be the one that presented the best tendencies response in the high-quality region of the workpiece, the lowest tool wear and the lowest force input in the process. To do so, a grading criteria and ponderation values will be given to the previous factors mentioned above in order to rank the experiment with the best performance and select the best lubricant.

## 2. Theoretical background

During this research, some concepts were performed for a better understanding of the reliability and software's involved and the help of specialists in the area was needed to guide and better understand the process it performs. Below are the necessary theoretical bases, concepts and definitions that support this project.

### 2.1. Blanking manufacturing process

It is a metal shearing process where a sheet material is sheared into a desired shape. In blanking the removed material (piece) is the final product and the sheet is scrap meanwhile in piercing is the other way around.

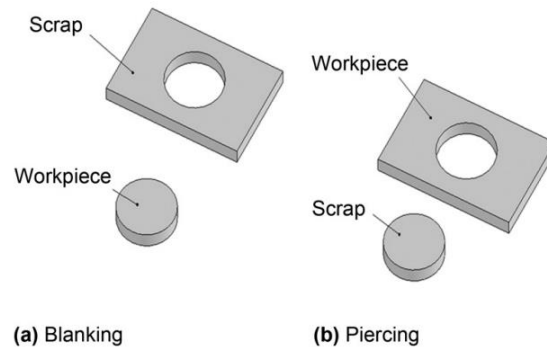


Figure 2-1 Blanking and Piercing schematic representation.

This process consists in different phases in order to deform and separate the sheet metal [1]:

- *Punch contact*: the punch first touches the fixed sheet.
- *Elastic and Plastic Deformation*: The punch starts to penetrate the sheet and cause elastic and plastic deformation.
- *Shearing and Crack Formation*: after high stresses, shearing occurs followed by fracture.
- *Breakthrough*: A large force would be necessary in the blanking process if the material has high strength or thickness. Compressive forces are stored in the tool and when fracture occurs these forces are released.
- *Stripping*: Punch is released and the part is ejected.

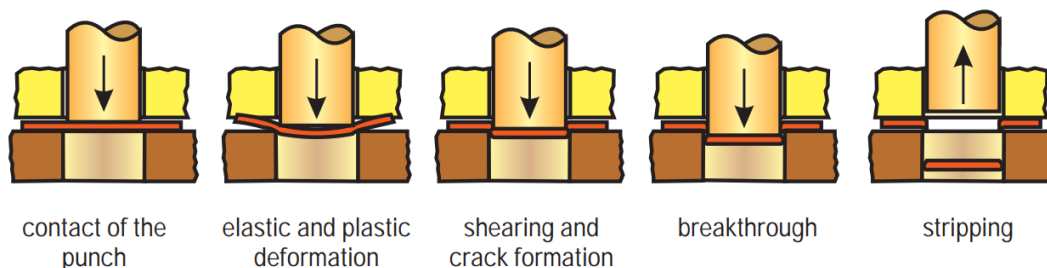
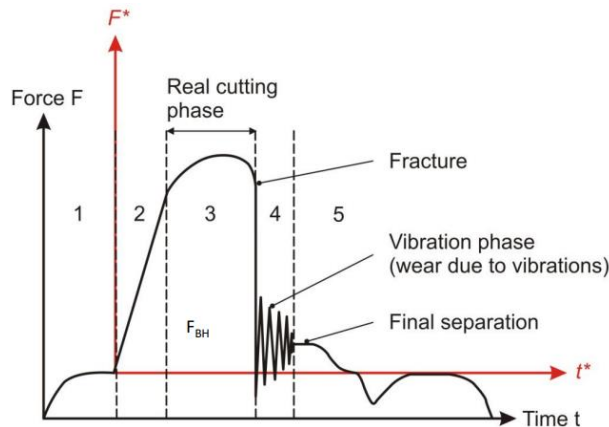


Figure 2-2 Phases of the blanking process. [1]

### Forces and Stresses.

The changes in the force signal can be investigated during the blanking manufacturing process. This force varies with the displacement, punch entry time and crack angel or punch geometry. The workpiece is evaluated in terms of regions formed along the cross section. Additionally, the cutting work (impulse) can be calculated by integrating the force over stroke [2]. The force signal can be investigated by different sections (**Figure 2-3**):

- Section 1: Punch move in.
- Section 2: The sheet metal deforms elastically.
- Section 3: Where plastic deformation occurs and strain hardening, which results in an increment of the cutting force up to the maximum load and crack starts to form.
- Section 4: Abrupt separation of the material and punch vibrations.
- Section 5: Collision with the die corners during return stroke.



**Figure 2-3** Force-time curve during the shearing process [3]

The equation that represent the resistance force to shear for a flat punch with ground working surface is the following:

$$F_s = A_s \cdot k_s = l_s \cdot s \cdot k_s \quad 2.1$$

$$F_s = 0.8 \cdot R_m \cdot l_s \cdot s. \quad 2.2$$

Where,  $R_m$  is the tensile strength in  $[N/mm^2]$ ,  $s$  is the material thickness,  $A_s$  is the sheared surface in  $[mm^2]$ ,  $l_s$  is the length of the sheared contour (perimeter) in  $[mm]$ , and  $k_s$  is the resistance to shear, shearing strength or relative blanking force of the sheet metal expressed in  $[N/mm^2]$ .

In order to reduce the maximum force need, the shape of the tool plays an important role. An Angle or stepped will lower the maximum force by spreading the work over a larger depth. The reduction in the maximum cutting force is attributed to both the shorter active cutting edge and the delay in the moment when the cutting edge comes into contact with the material. In the **Figure 2-4** a visual representation of the force signal influenced by the shape of the tool can be seen.

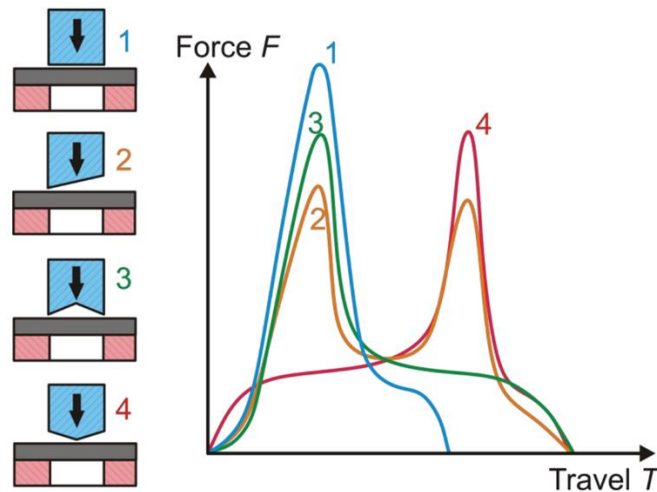


Figure 2-4 Cutting tool edges [3]

**Different zones of a workpiece:**

After cut, the workpiece has different remarkable areas or zones that can be observable. The ratio of this different zone is influenced by different parameters, such as clearance, material properties, shape of the cutting tool, etc. In general, a larger shear zone is preferable. Following, the different zones are described and its visual representation can be seen in **Figure 2-5**.

- *Rollover zone ( $Z_r$ ):* Caused by plastic material deformation.
- *Shear zone ( $Z_s$ ):* Smooth and shiny area created during material shearing.
- *Fracture / rupture zone ( $Z_f$ ):* rough surface, results after breakage.
- *Burr zone ( $Z_b$ ):* Caused by plastic deformation.
- *Depth of crack penetration ( $D_{cp}$ ):* angle of fracture zone, depends mainly on clearance.
- *Secondary shear:* Created if cracks do not run toward each other and material is sheared again.

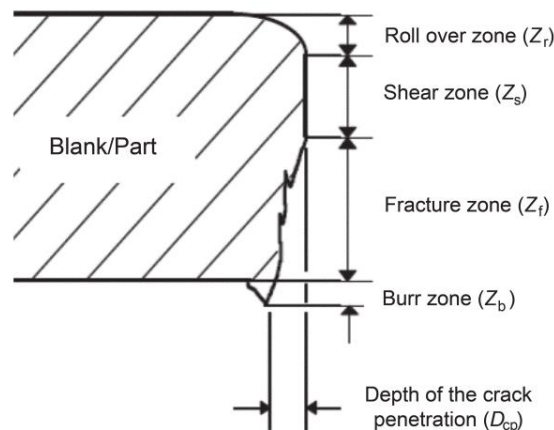


Figure 2-5 Different zones if the balked workpiece cross section [2].

### Factor affecting the quality of the workpiece:

- *Material Properties:* Ductile materials are preferable due to more plastic deformation and hence more shear zone than brittle materials. The material thickness and shear strength also affect the force required to shear.
- *Hold-down force:* ensures that the material remains on the table and does not lift during shearing.
- *Shearing velocity:* higher shearing velocity gives better shearing edges.
- *Tool material:* the material is selected according to the number of parts to be blanked. Typically used: tool steels, cemented carbides, steel-bonded carbides or powder metallurgy tools. High speed tool steel provides smaller burr zones. Carbides give longer tool life than tool steels.
- *Clearance:* The punch wear is greatly influenced by the clearance between punch and die. Smaller clearances induce greater punch forces. There is an optimum clearance for which punch forces and the minimum based on the properties and thickness of the material blanked [2].

### Failure modes of the tool:

The most important factor when studying the failure modes is the relationships between the strength of the workpiece and the hardness of the cutting tool.

- Adhesion wear: Material added onto the surface of the punch from the workpiece material.
- Abrasive wear: Normally in high-strength steels, produces deterioration of the surface of the tool by removing material.
- Fatigue wear: Continuous circulation stroke loading. Can produce tool failure.
- Oxidation wear: It occurs when exposing the tool to corrosive environments such as air, or excess lubricant that has not been cleaned, in combination with changes in temperature and working medium, which causes oxidation and deterioration of the tool [4].

### Fine Blanking

Aim to manufacture parts with a smooth sheared surface. The material is blanked only by shear and not fracture after being clamped on all sides. These results in lower vibrations and noise but with higher tooling cost and smaller cutting speed are required. The die clearance for fine blanking is approximately 0.5-1% of the blanking thickness [2] (see **Figure 2-6**).

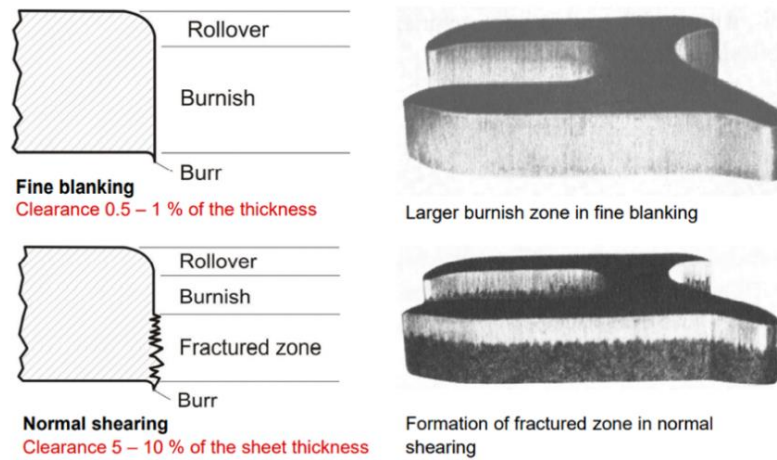


Figure 2-6 Fine blanking and normal shearing comparison [2]

## 2.2. Fast Fourier transform

Fast Fourier transform (FFT) is a discrete Fourier transform algorithm of high importance used to analyze force, acoustics and audio signals measurements. It converts the signal inputs into individual spectral components of amplitudes and related frequencies. Fast Fourier Transforms (FFTs) are employed in the examination of faults, the supervision of quality, and the monitoring of the condition of machines or systems. The discrete Fourier transform is defined by the following equation 2.3.

$$X_k = \sum_{n=0}^{N-1} x_n \cdot e^{-\frac{2i\pi kn}{N}} \quad k = 0, \dots, N - 1 \quad 2.3$$

Where  $x_0, \dots, x_{N-1}$  are complex numbers and  $e^{\frac{i2\pi}{N}}$  is a primitive  $N_{th}$  root of 1. This discrete Fourier transform reduces the number of computations needed for  $N$  number of points from  $2 \cdot N^2$ , where there are  $N$  outputs  $X_k$ , and each output requires a sum of  $N$  terms, to  $2 \cdot N \cdot \lg(N)$  where  $\lg(N)$  is a base 2 logarithm [5].

In the **Figure 2-7** it can be seen how is the visualization of the decomposition of the signal in amplitude and frequency values. In order to perform this method with measuring devices a sampling frequency  $f_s$  must be established, which are the number of samples that can be obtained per second.

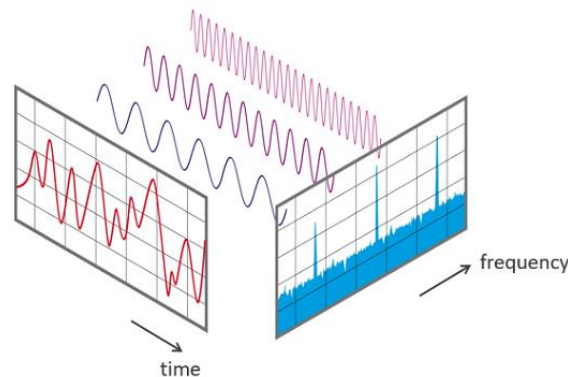


Figure 2-7 Signal decomposition representation in the time and frequency domain. [6]

### 2.3. Power spectrum analysis

Power spectrum analysis is a technique commonly used, which consist in applying fast Fourier transforms (FFT) of a particular signal and take its amplitudes and multiply them by its complex conjugate over its frequency spectrum, which results in the real only spectrum of amplitude. The result is presented as a plot of signal power against frequency, which is called power spectrum. It indicates the relative magnitudes of the frequency components that combine to make up the signal [7].

The signal is ideally expected to have random excitation in order to generate appropriate data. It is commonly used to determine the degree of noise that is associated with the signal and deciding on appropriate sampling rated. This term refers as well to the spectral energy distribution that could be found per unit time. The integration of summation of the spectral components will lead to the total power contained in the signal (Eq. 2.4)

$$E \triangleq \int_{-\infty}^{\infty} |x(t)|^2 \cdot dt = \int_{-\infty}^{\infty} |\hat{x}(f)|^2 \cdot df \quad 2.4$$

Where,  $E$  is the energy,  $x(t)$  the signal,  $\hat{x}(f)$  is the value of the Fourier transform of  $x(t)$  at frequencies  $f$  in (Hz).

### 2.4. Blanking manufacturing machine:

To perform each set of experiments, the TruPunch 5000 was used which is a blanking manufacturing machine that is present at the IUL facilities at the TU-Dortmund. This machine is capable of 1600 strokes/min and up to 2800 strokes/min and can provide high process reliability and flexibility up to the new productivity standards. It is capable of fast tool change and multitool application with automation capability.



**Figure 2-8** TruPunch 5000 blanking machine. [8]

## 2.5. Profilometer

Device, which uses state of the art white light interferometry to measure surface roughness and geometry dimension, profiles of different workpieces. During this investigation, it was used to measure the development of the different profile sections presented in the workpiece and geometry related fatigue development of the punch after blanking, such as roughness.

These optical measuring machines have an important advantage over tactile measuring devices. It can allow components to be measured directly on the measurement bed without the need for alignment. In addition, some of the advantages are the speed of the measurement; optical measurements are faster than tactile ones, by avoiding deformations in the components and making it possible to obtain measurements for which the probe of tactile devices is too large [9].



**Figure 2-9** Keyence optical measuring machine

### **3. Literature review.**

Blanking process is a widely manufacturing process used in sheet metal forming and often combines other several forming operations as intermediate or post processing step. In blanking, new surfaces are generated by means of material shearing and during this process; frictional stresses are exerted of the punch stem during backstroke force creating severe tribological conditions. Some materials like stainless steel have high affinity for adhesion with steel tools, therefore prone to cause local pick-up on the punch stem, tip and surfaces.

This add up materials affects the workpiece quality and the increases the tool wear in the subsequent strokes by introducing larger tensile stresses in the punch and thus higher forces that can lead to tool failure. According to Lind [10], the wear mechanism occurring in a blanking process is characterized by three distinct phases where abrasive wear, adhesive wear and growth of friction junctions are respectively dominant. Olsson [11] conducted extensive investigations on wear and lubrication in punching. The studies showed that the mechanism of lubrication in punching is governed by the lubricant retained on the surface of the punch stem and by the chemical interaction of the lubricant additives with the punch and sheet material [12]. It was found that a tangential texture on the punch surface combined with a high viscosity lubricant reduced the amount of wear developed on the punch surface during testing [13]. Additionally, the research demonstrated that the increase in backstroke force as the number of strokes increased provided valuable insight into the extent of wear occurring on the punch stem. It was also found that for the punching test, lubricants containing robust boundary films were necessary to prevent excessive wear on the punch stem [14].

Blanking processes exhibit severe tribological conditions, where insufficient lubricant quality leads to heavy pick-up material of the workpiece to the punch, resulting in poor surface quality of the final product, reduced dimensional accuracy, shortened the tool life and increasing the force values. Therefore, during this study, the effects of different types of lubrications in the previously mentioned aspects are going to be investigated and how do they behave as the number of strokes increases.

#### **3.1. Machine learning**

It is a set of algorithms and statistical learning and optimization methods used in data analysis that imitates the behavior and can automatically detect data patterns in order to predict future data or to perform decisions under uncertainty. According to Arthur Samuel, machine learning enables computers to learn and improve on their own without the need of additional programming. These methods could be used in Artificial Intelligence (AI) in order to imitates intelligently, human behavior [15].

Machine learning can be structured in three main components [16]. A Decision Process, which uses labeled or unlabeled input data in an algorithm that can estimate patterns in data sets. An Error function evaluates the prediction made by the model by comparing previous examples if existed to assess accuracy of the model. An optimization process that weights and adjusts the model for better fitting by updating these weights autonomously until the threshold of accuracy has been met.

The field of machine learning has developed different types of algorithms that can be used to address multiple applications. According to the nature of the problem, a specific type of algorithms can have a better fitting and resemble the results with high level of accuracy. Within this investigation, Gaussian Process Regression will be the algorithm used to estimate the behavior of the variables involved.

### 3.1.1. Gaussian process regression (GPR)

It's a mathematical tool used in statistics, which provides uncertainty measurements on predictions from a nonparametric kernel-based probabilistic models. Gaussian process is a stochastic process, where each group of the random variables has a multivariate normal distribution and every finite linear combination of them is normally distributed. Its main distribution is the joint distribution for all the random variables.

For instance, for each set of data points, GPR resembles every entry  $x$  as a vector function  $f(x)$  and infer properties of the function by means of the finite number of data points and thus, make predictions. This function, that goes through all of observed data points, is given a prior probability distribution with GPR (Eq. 2.5) [17].

$$f(x) \sim GP(m(x), k(x, x')) \quad 2.5$$

Where,  $m(x)$  is the mean function and  $k(x, x') = Cov[f(x), f(x')]$  is the covariance or kernel function between any two functions  $f(x)$  and  $f(x')$ .

These parameters can be tuned to fit specific physical problems, and thus GPR can be optimized. The kernel function captures the inherent structure within the data by quantifying the similarity between data points, which are stored in the covariance matrix and represent the interrelationships between different points in the dataset. GPR becomes then very versatile but dependent of the covariance function selected, allowing for a wide range of models to be specified. For this investigation, the Squared Exponential (SE) Kernel function will be used which is the most frequently selected in machine learning applications thanks to the easy integration against most of the functions. Squared Exponential Kernel is defined by the following equation 2.6.

$$k_{SE} = \sigma_f^2 \cdot \exp\left(-\frac{(x - x')^2}{2l^2}\right) \quad 2.6$$

Where,  $l$  determines the length of the wiggles in the function, and  $\sigma^2$  is the output variance [17].

## 4. Problem definition

### 4.1. Methodology and experiment details

#### Experiment designation and structure:

The blanking experiments consisted of the use of four punches, one without lubricant and the rest with each a different type, to perform 24700 strokes each divided in sets of 988 for a total of 25. Each set consisted of 13 rows of 76 strokes (as it can be seen in the **Figure 4-1**) and within each set, the force signal over time and measurements such as wear development of the tool and quality of the samples were obtained. For the study of the workpiece's quality evolution, in the first and last row of each set respectively one sample of these rows was collected for a total of 50 samples for each punch. Subsequently, the samples were measured by the profilometer, my means of a holder, to obtain cross section dimensions and roughness evolution (see **Appendix A**).

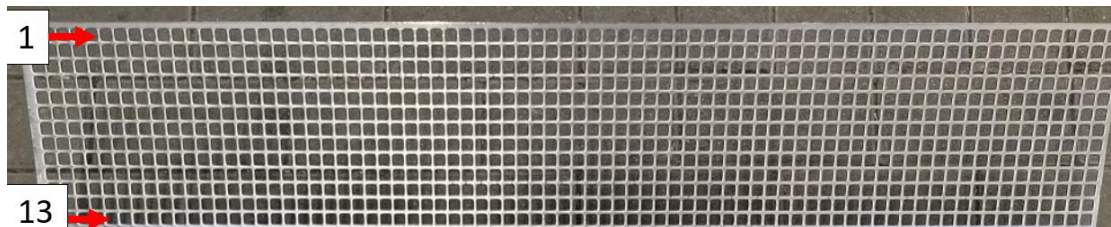


**Figure 4-1** Set and rows representation

#### Punch dimensions and theoretical force:

The conduction of this research was held using four square geometries punches with side dimensions of  $a = 10 \text{ mm}$  for the first three and a dimension of  $a = 9 \text{ mm}$  for the last one (**Figure 4-2**). This geometry facilitates the study of the wear behavior of the tool and the quality evolution of the workpiece since it has rectangular angles and the results could be better visualized with the profilometer, which is the machine, used to measure the results. Other punch geometries do not provide these advantages and would lead to measurements failures and percentage errors, for instance, with a circular punch, the cutting edge angle can only be measured at one point of the circumference at a time and not several measurements along a side like for example in case of a square punch. Furthermore, in order to obtain the most visible tool wear evolution, the tip of the punch was chosen to be flat, thus only right angles are present.



**Figure 4-2** Square punch.

### Metal Sheet material:

The material chosen for this blanking manufacturing process was the DC04, which is a steel mostly used in deep drawing and provides good mechanical properties, such as good deformability and high strength that can facilitate the measurements with the profilometer. On the other hand, either a really ductile material or a highly brittle material would complicate the quality of the results, since the evolution can be shortened due to fractures located at the metal sheet, faster wear development of the punch (in the case of brittle materials) or high deformed workpieces (case of really ductile materials). Finally yet importantly, for thinner sheets the measurements would be harder to visualize at the cross section. The thickness chosen for these experiments is  $s = 3 \text{ mm}$ . The mechanical properties of this material are listed below in **Table 4-1** [18].

**Table 4-1** Mechanical properties

Yield strength Re (MPa)	210
Tensile strength Rm (MPa)	270-350
Elongation at fracture % min.	38
Anisotropy r90	1.6
Strain hardening exponent n90 min	0.18

### Lubricants:

In this research, the lubricants and the designation of the punches within this study can be seen in the following table (**Table 4-2**). Due to non-disclosure agreement (NDA) the full name, chemical and physical properties and the selection of these specific lubricants cannot be displayed.

**Table 4-2** Experiments designations

Experiment designation	Lubricant
Punch 1	unlubricated
Punch 2	FN 6870-38
Punch 3	FN 4455-55
Punch 4	W-A

### Theoretical force calculation:

According to the manufacturer, the theoretical force can be calculated by means of the following equation (Eq. 4.1). Given the experiment specification and data provided by the manufacturer in their operating manual [19].

$$F = \frac{4 \cdot a \cdot s \cdot \sigma}{X} \quad 4.1$$

where,

$a$  = Side length

$s$  = Sheet thickness

$\sigma$  = Tensile strength

$X$  = Shear factor

Given the experiment specification and data provided by the manufacturer in their operating manual, the theoretical force can be calculated [19].

$$F_{Punch} = \frac{4 \cdot (10 \text{ mm}) \cdot (3 \text{ mm}) \cdot \left(350 \frac{\text{N}}{\text{mm}^2}\right)}{1} = 42 \text{ kN}$$

### Force input data:

The force values of the experiments were calculated indirectly with the following equation (Eq. 4.2), since the transmitters presented at the machine only measure the pressure inputs of the two chambers set (see **Figure 4-3**). In the figure can be seen the “Upper pressure chamber A1” and “Lower pressure chamber B” connections in the machine.

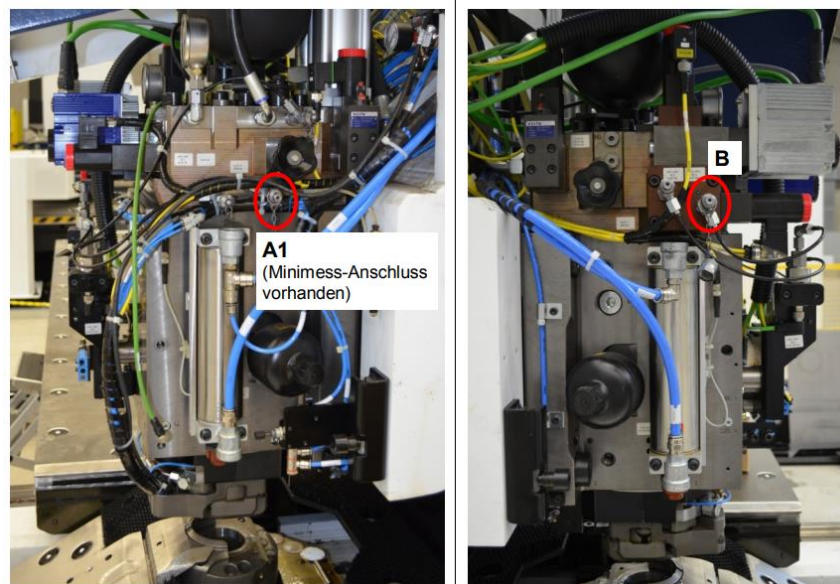


**Figure 4-3** Measuring points on the punching head for measuring the punching force

The manufacturer provided the following equation and the measuring parameters (See **Table 4-3**).

$$F = 0,1 \cdot (p_{A1} \cdot 9776 \text{ mm}^2 - p_B \cdot 4661 \text{ mm}^2) \quad 4.2$$

where,

$F$  = Force [N]

$p_{A1}$  = Pressure at cylinder A [bar]

$p_B$  = Pressure at cylinder B [bar]

**Table 4-3** Measuring parameters

Sampling frequency	19200 Hz
Filter type	AAF
Filter characteristic	Butterworth
Data type	16-bit integer

### **Force data handling and calculations:**

In order to analyze the force signal and calculate the PSD and Impulse evolution, the acquired data had to be handled in a proper way to obtain the desired results.

- First, each set was analyzed and cleared from any dead time during the experiments, i.e. unnecessary or unplanned stops that will contaminate the signal. This involves cutting the signal and merging with the rest when no strokes are being made.
- Secondly, after performing the same procedure with all of the sets, a total force vs time signal was obtained for each experiment after merging the sets together.
- Finally, since the aim of this investigation is to study how the force signal evolves along every stroke, the total force signal of each experiment was divided so each stroke can be studied individually.

### *Frequencies and power analysis:*

Now, by having every corresponding stroke of each experiment, the FFT and PSD evolution can be performed and plotted. The FFT was used to study the amplitudes and the frequencies of the signals and compare their behaviors to see if it follows any pattern between them. It was also studied if new frequencies do appear after a specific number of strokes at higher frequencies in a 3D plot, which will indicate that unwanted vibrations are being present that could lead to tool wear, material deformation and high-energy consumption.

Additionally, a set of frequencies intervals of the FFT spectrum were established and the peak frequency evolution among each stroke was studied. The peak frequency provides relevant information about the signal's characteristics and underlying the process. For instance, the peak frequency can help to identify the primary oscillation, vibration mode or resonance of the system, which can later be beneficial to adjust damping conditions of the system, that for this case means better cutting condition. Besides, the study of the peak frequency can also help monitor the system and act as an early warning for faults or deterioration in machinery, enabling timely maintenance and minimizing downtime.

The PSD, on the other hand, was used to obtain the energy contained in every stroke by means of its integration. Each result of every stroke represent a point in a scatter graph which then was used to obtain the machine learning regression of the whole experiment by means of GPR and linear regression. Furthermore, the sum of each result provides the total amount of energy for each experiment, so a clear comparison can be made with these results to determine the best lubricant. In **Figure 4-4** the workflow of this study can be seen for better understanding.

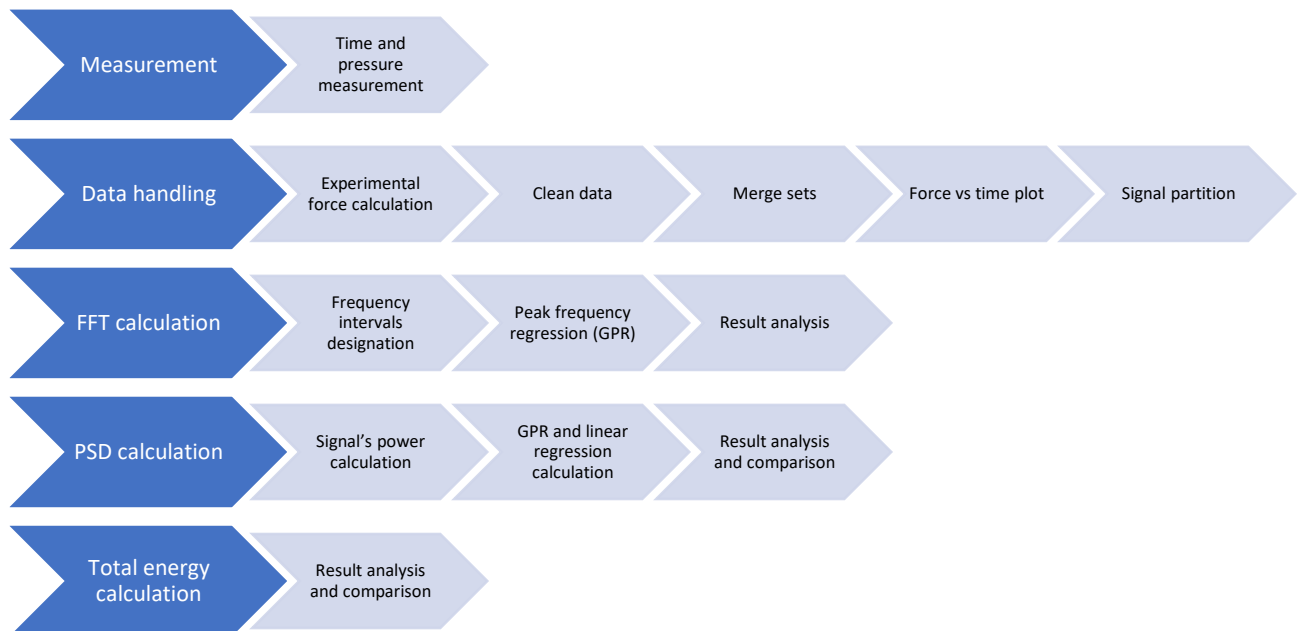


**Figure 4-4** Frequency and power analysis workflow

Impulse calculation:

This same procedure was also carried out to evaluate the impulse evolution of every stroke in time, which is the integral of the force per unit of time (See Eq. 4.3), in this case, per stroke, also called cutting work.

$$I = \int_{t_1}^{t_2} F \cdot dt = \int_{v_1}^{v_2} m \cdot dv \quad 4.3$$

Each result corresponding to each stroke of every experiment was then compared by means of the total impulse involved and its behavior in time was approximated by means of GPR and linear regression. The workflow of this calculation procedure can be seen in **Figure 4-5**.

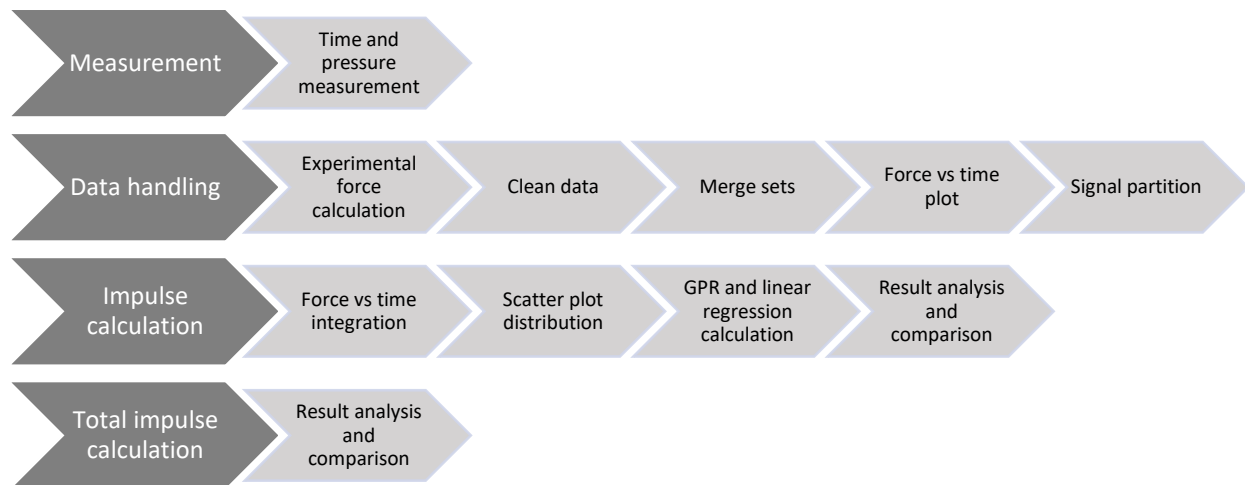


**Figure 4-5** Impulse calculation workflow

**Tool wear:**

The expected measurements involved in this analysis were obtained to calculate the edge radius and the roughness development of each punch side surface.

Edge radius wear evolution:

The methodology followed was to acquire five measurements (with the profilometer) of the edge radius of every side of the punch starting from the middle and spreading four more along the edge but avoiding the corners to then average it. The measurements were held at an angle of 45 degrees. This methodology was performed at the beginning of every experiment, i.e., without wear, and then for set 1,3 and 5, subsequently for every 5 sets until reaching set number 25. In the **Figure 4-6** shows how the measurements were conducted along each edge and how the profilometer perform each measurement from the image acquired.

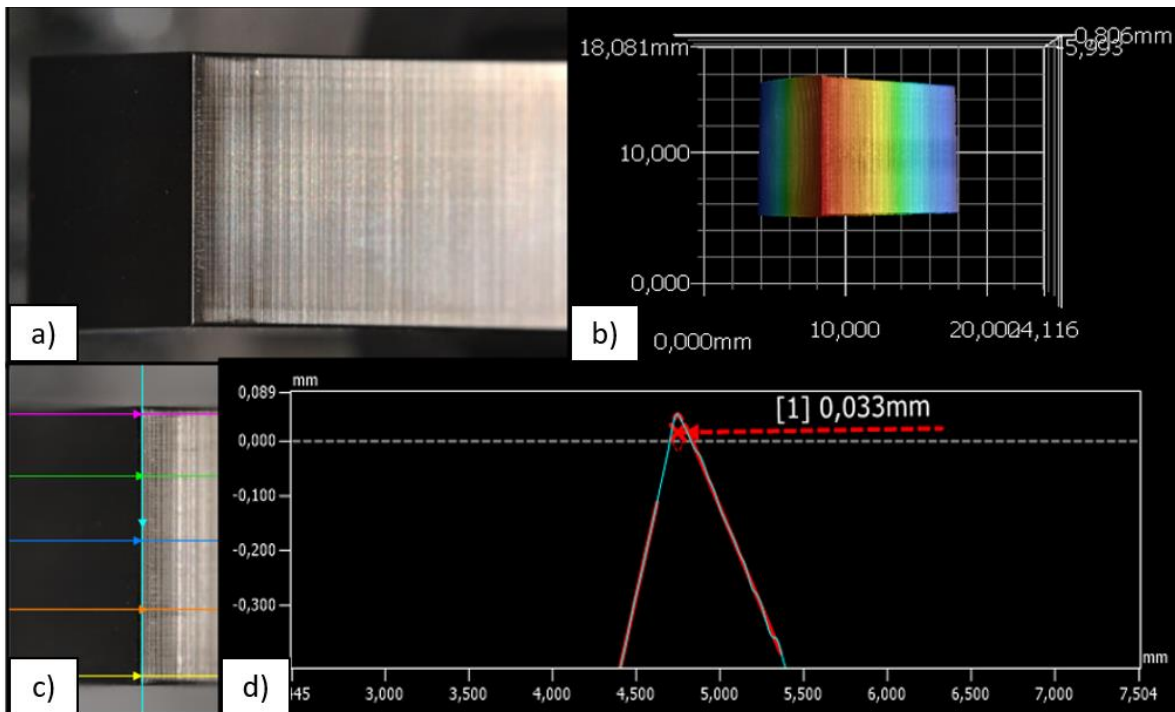


**Figure 4-6** Edge radii measurements, a) Punch at 45 degrees b) 3D surface representation, c) Measurement lines representation, d) Edge radius

The cutting-edge radius is a key criterion for assessing tool wear, since blunting of the cutting edge leads to poorer edge quality on the workpiece and is therefore crucial when it comes to re-sharpening. In addition, the changes at the cutting edge and punch area have a direct influence on the force behavior.

Roughness depth  $R_z$  evolution at punch surfaces:

The punch surfaces roughness depth was also considered to evaluate the wear of the tool. It is expected that for higher number of strokes, more surface wear will be experienced and thus, material loss at the surface of the tool. This material loss or wear volume, as described before, could not be clearly determined since build up material occurs while performing the blanking process which means that the debris of the of un-machined part get adhere to the surface of the punch. This build up material, will have an effect in the tool by decreasing the wear measurement of the material loss and the results will not be reliable.

It is important to notice that this abrasion and adhesion are occurring simultaneously while performing the blanking process and its behavior may vary. In the **Figure 4-7** it can be seen, how the surface of the punch looks after 24700 of strokes.

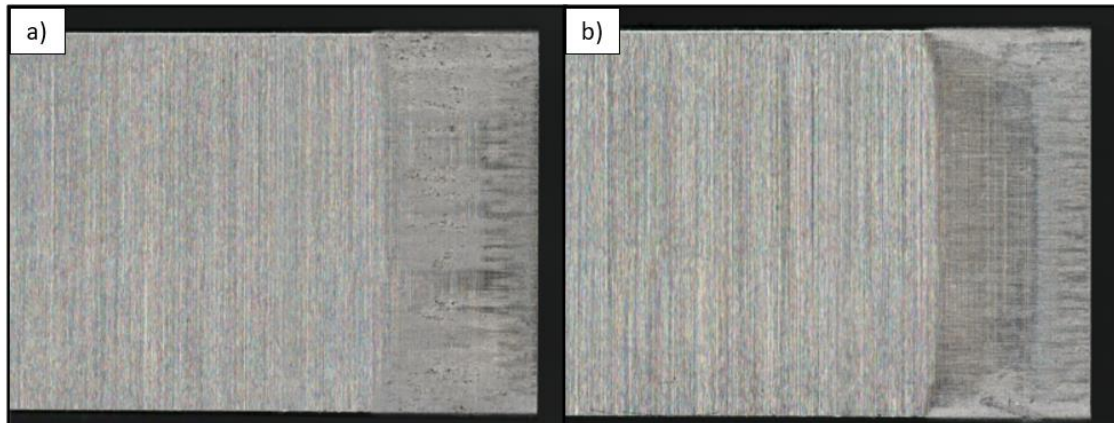


**Figure 4-7** Comparison at the punch surface quality after a) 988 strokes and b) 24700 strokes for punch 1.

From the previous figure, the wear of the tool can be clearly seen already after 988 strokes, nevertheless, the adhesion occurs along the surface of the punch. A clear surface can then be seen again after 24700 strokes, this indicates that the buildup material was then carried out of the surface. It is noticeable that two sections can be clearly identified from the picture and its division correspond to the part of the tool that does the cutting (the cutting edge) and the other that has contact with the sheet after cut. In the first section, more abrasion can be seen while in the other section more adhesion, however, as mentioned before both events occurs simultaneously therefore, the roughness parameters were measured as indicator of wear since the abrasion and adhesion do not cancel each other.

The methodology implemented to carried out this study, was to perform eight measurements sections perpendicularly to the punch side length, parallel to each other (See **Figure 4-8**) and for all four sides, and along the whole width. These measurements were conducted at the same set intervals as mentioned before in the case of the edge radius, and contained eight lines where roughness was determined. The values obtained for every roughness section were then averaged to get the correspondent roughness value for that number of sets.

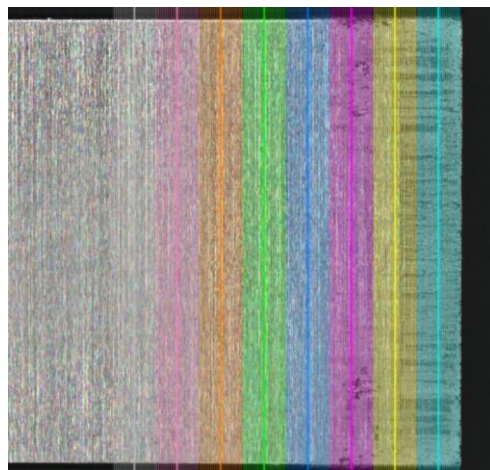


**Figure 4-8** Roughness measurements

It is important to notice that, to get a more certain value of the roughness, the edge values were not included so the variance of the measurement will not increase by adding additional error and for the existing radius of edge wear to affect the procedure.

**Workpiece quality:**

The expected measurements involved in this analysis were obtained to calculate the roughness evolution and the cross section development.

*Shear zone roughness evolution:* It was measured as an indicator of the shear strength experienced by the workpiece. A high roughness would lead to more post processing in the manufacturing process, which will increase the cost of production by means of time and labor cost. Depending on the nature of the product and either is fine blanking or normal shearing; this aspect will be relevant for quality control in production. In the **Figure 4-9** it can be seen how the measurements were held by means of the profilometer and how the surface profiles were captured.

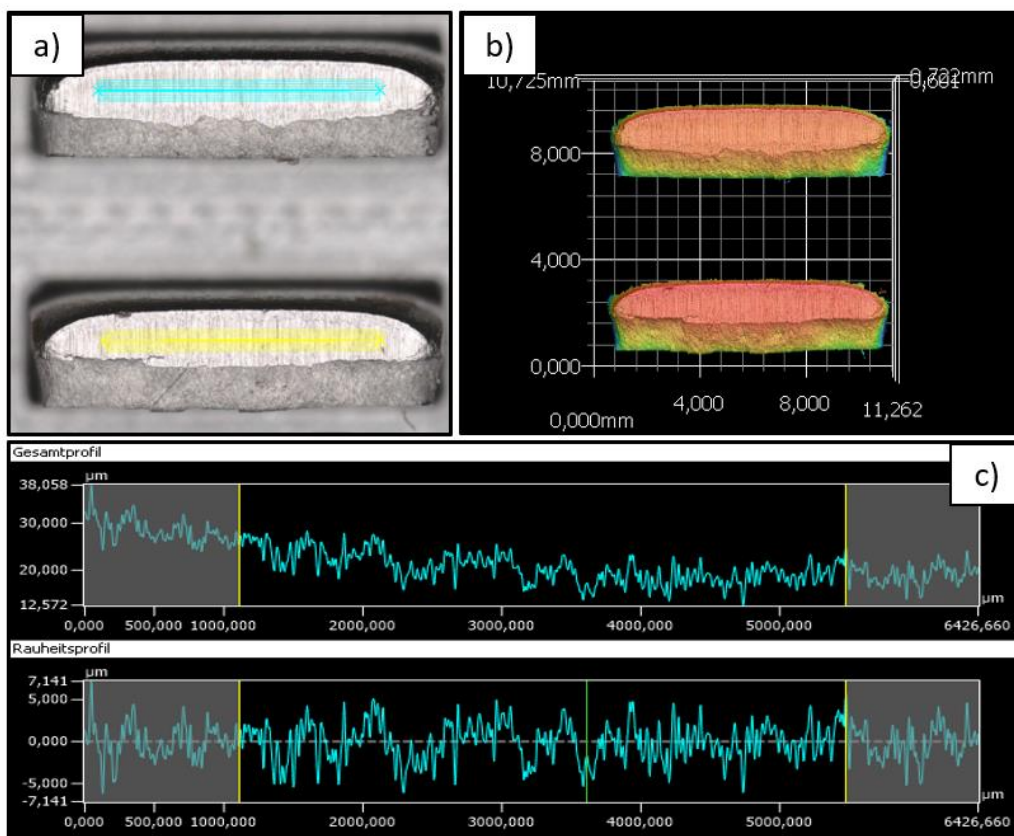


**Figure 4-9** Roughness sample measurement. a) measurement length, b) 3D surface representation, c) roughness profile.

Following the previous criteria, the roughness measurement was held at the middle of the burnish zone, where the shear strength occurs. The fracture zone was not taken into consideration since the roughness

value does not represent a great significance since the aim of these manufacturing processes is to obtain the best quality product to minimize the post processing and the cost involves within the production chain but only its height dimension is relevant for these studies.

*Cross-section evolution:* the dimensions of the workpiece's samples were measured at the highest value related to each of the sections. Since the dimensions of each section varies along each of the sides, the most homogeneous side was chosen and the measurement performed in the middle, where it normally was seen the highest value of the burnish zone as it can be seen in **Figure 4-10**.

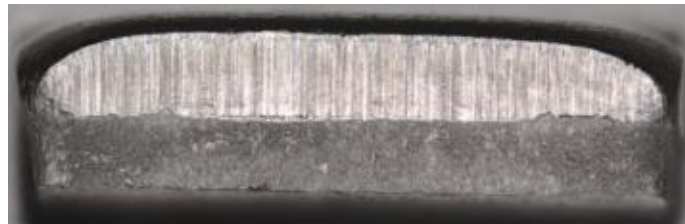


**Figure 4-10** Sample cross-section

The dimensions measured were the shear zone height and the fracture zone. The sections fracture and burr were taken into consideration as a whole (see **Figure 2-5**) and the rollover zone calculated indirectly from the other dimensions and the original sheet thickness (**Figure 4-11**).

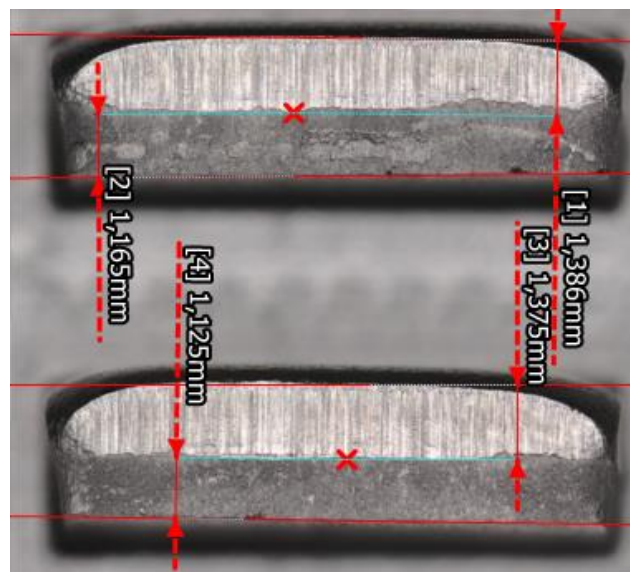


**Figure 4-11** Sample cross-section measurements.

The most visible comparison that can be observed and the most relevant section to study is the shear zone height. When the shear zone height decreases, it is understood that the plastic deformation also does and thus the workpiece is being fracture at the cross sections and not actually cut.

### Ranking and grading:

In order to determine which experiment had the best and desirable results, and establish whether to use or not lubrication in the blanking process, a ponderation factor was given to each of the parameters regarding the samples, punch and force evolution (according to **Table 4-4**) with a grading factor (according to **Table 4-5**), according to the following equation (Eq. 4.4).

$$R = \frac{\sum P_{vi} * G_{vi}}{\sum P_{vi}} \quad 4.4$$

Where:

$P_v$  : Ponderation value

$G_v$  : Grading value

**Table 4-4** Ponderation Values

Ponderation Value	
1	Ordinary
2	Relevant
3	Most relevant

**Table 4-5** Grading criteria

Evaluation Value	
1	Best
2	Normal
3	Regular
4	Worst

The grading will be evaluated in three main aspects, force (Power and impulse evolution), tool wear (Edge radius and roughness surface evolution) and workpiece (Roughness and cross-section evolution). The criteria used to assign the rating was, the best scenario among the experiments obtains rating 1, for similar results the next rating will be repeated and the least probable or expected result will be assigned the immediately following rating.

## 5. Experimental results

### 5.1. Force signal

After gathering the data from the experiments and inputting the values to obtain the correspondent forces values, a plot displaying the force vs time was obtained, such as in **Figure 5-1** for every punch. To get a proper analysis of the development of the force in detail, each stroke was studied individually, in the **Figure 5-2** the force vs time plot can be seen for a single stroke for punch number 1.

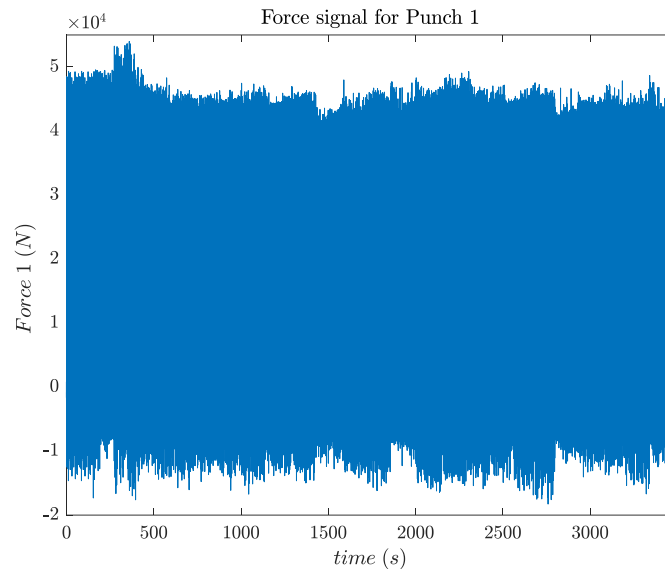


**Figure 5-1** Force signal related to punch 1

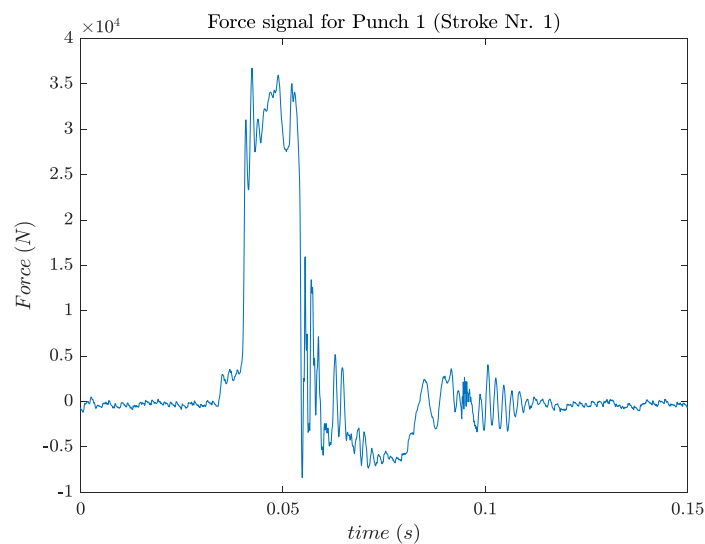


**Figure 5-2** Single stroke. Force signal for punch

The approximated period of every stroke was about 0.15 seconds and for a total of 148,2 seconds per set, the shape of the signal and the maximum force value was 10 % smaller than the theoretical one of a square punch such as in the Eq. 4.1 In the **Figure 5-3** the FFT of the stroke number 1 for punch 1 can be seen, following the evolution of the FFT a long every stroke of the experiment in **Figure 5-4**.

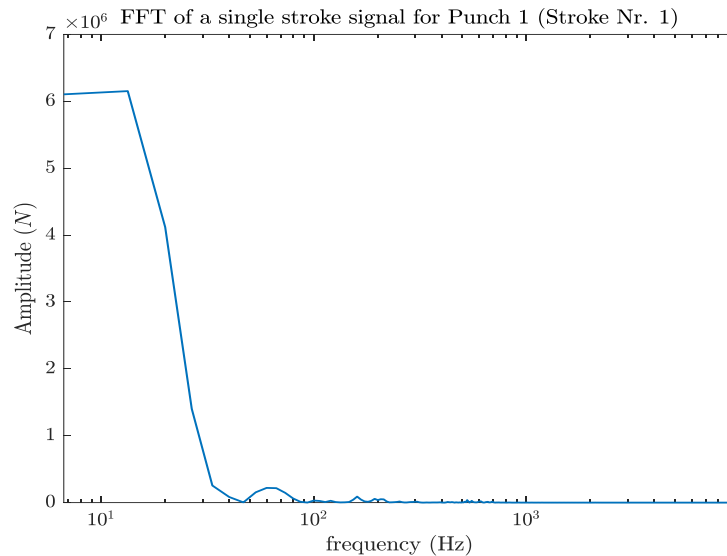


**Figure 5-3** FFT of a single stroke. Punch 1

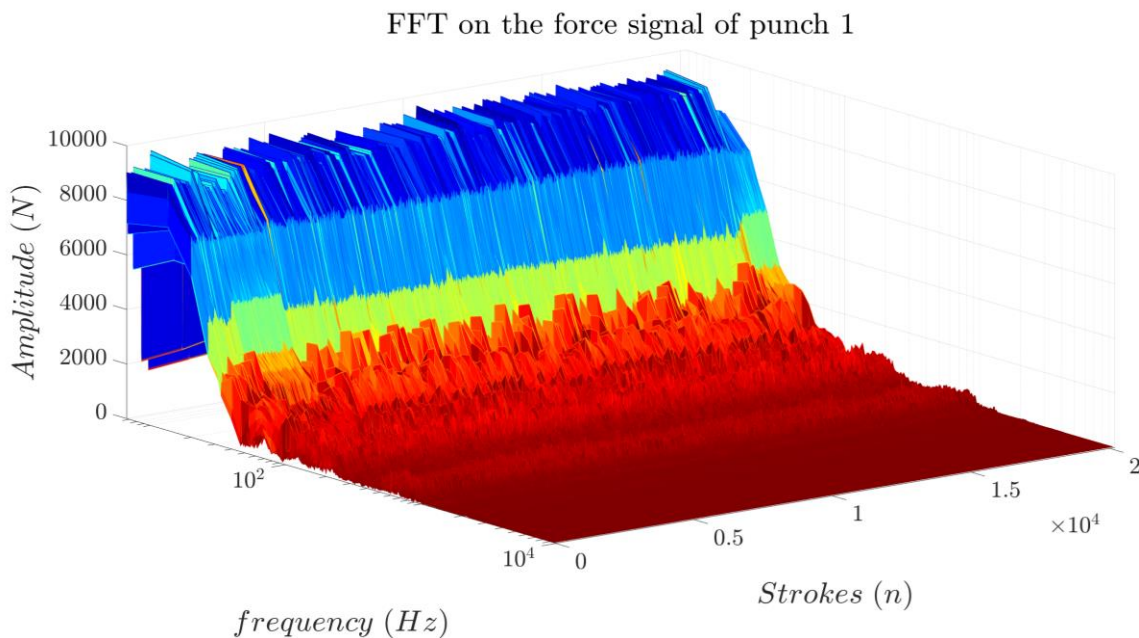


**Figure 5-4** FFT evolution along each stroke

This procedure was performed for each of the punches (see **Appendix B**). For a better comparison, a plot of the FFT of the first stroke of each punch was carried out to see how the frequencies behave and in which range they occurred. In **Figure 5-5** it can be seen that for the punches 1,2 and 3, the frequencies of the spectrum lays within the same interval along its range, but not for the case for punch 4 since its dimension is smaller than the other punches.

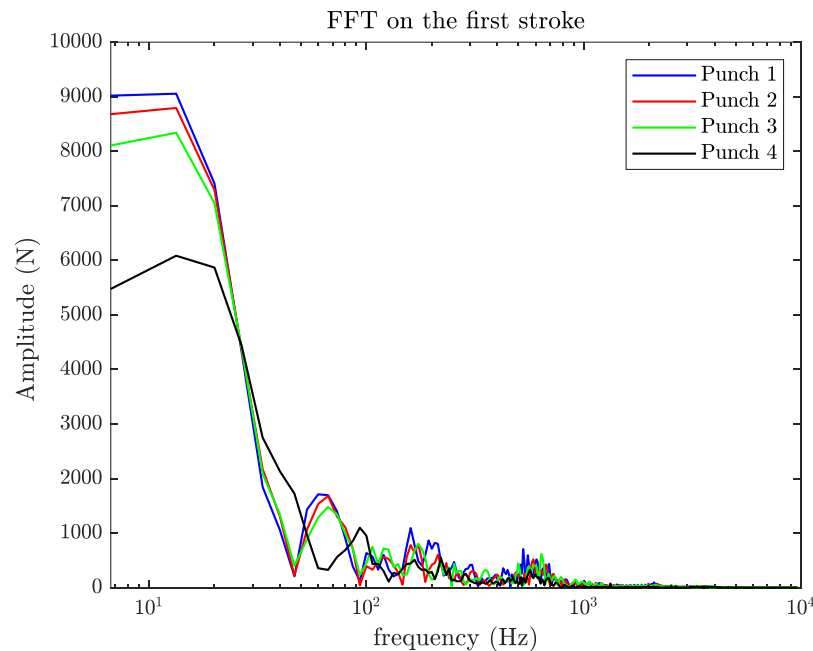


**Figure 5-5** FFT comparison of every experiment at the first stroke.

Furthermore, in order to analyze how the frequencies behave for every stroke in time, the set of intervals established to study the peak frequency evolution within each range for each experiment can be seen in **Table 5-1**. Additionally, in order to obtain the behavior in time of these peak frequencies, a Gaussian Regression Model was performed. The evolution of each peak frequency within each interval, can be seen in **Figure 5-6**.

**Table 5-1** FFT frequency intervals

	Interval (Hz)
f1	0-47
f2	47-133
f3	133-265
f4	400-700

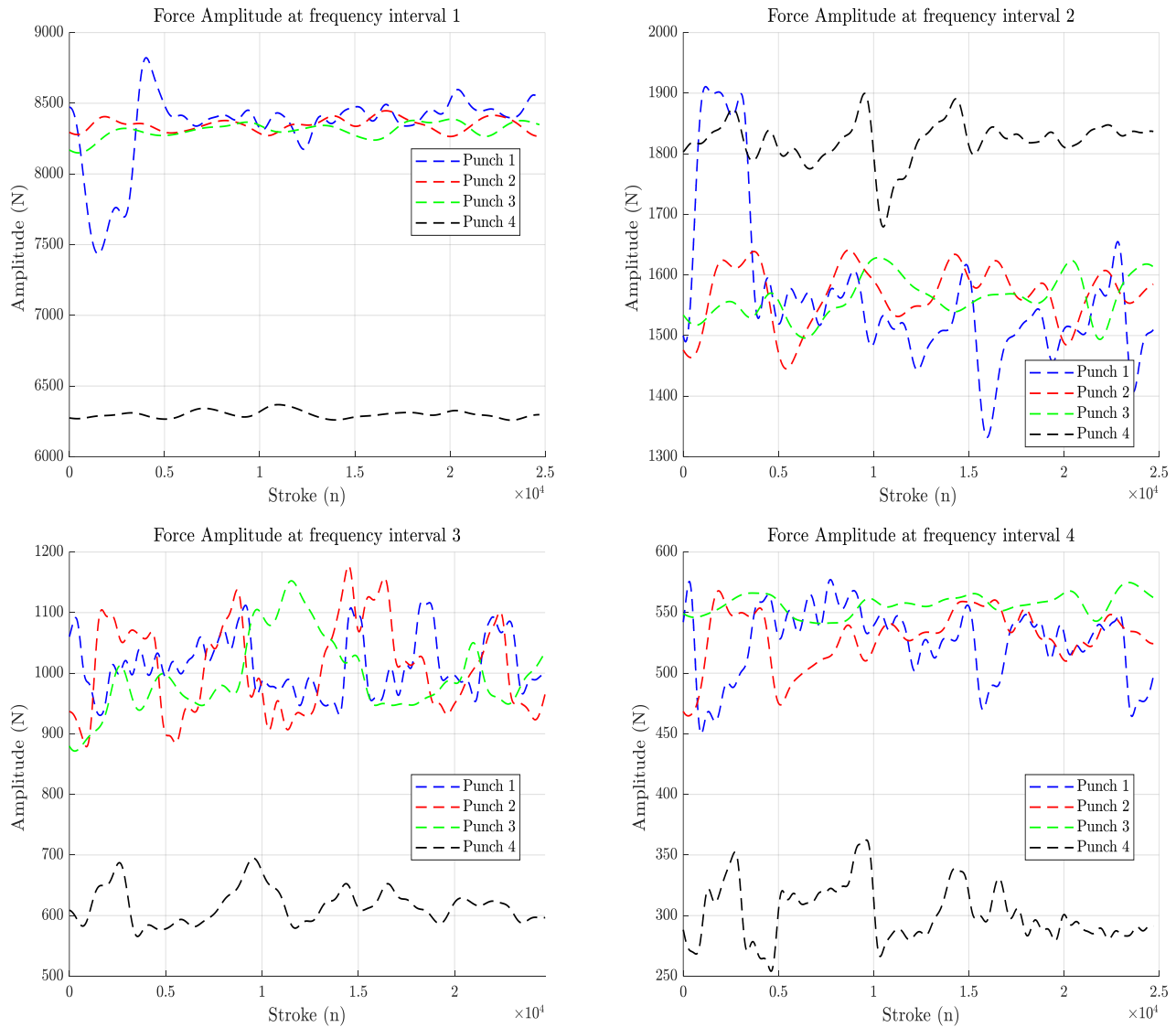


**Figure 5-6** Peak frequency intervals evolution

From the previous **Figure 5-6**, it can be seen that for punch 1 to 3, the behavior of the peak frequency lay within the same amplitude values but not for punch number 4. These results were expected since this punch has a 9 mm side dimension while using the same 10 mm square die as the other experiments, this mean, that less force is needed to perform the process and thus the amplitudes of the frequencies vary and does not correlate with the others. For punch 2 and 3 the low frequency behavior, were most of the signal is contained, follow similarly the same pattern as the dry punch, punch 4 also does it but at lower amplitudes.

Furthermore, for punch 1 in the intervals 1 and 2 a strong decrement and a high increment can be observed respectively at small number of strokes, but it follows a more stable state as the experiment develops. This

behavior could be described as the initial tool wear that lead to changes in the interaction between the tool and material (can be later seen at page 34 in tool wear results), some minor initial wear can be also seen for punch 2. Another explanation is the temperature conditions, since the punch 1 in unlubricated, the heat produced by friction before reaching stable level and wear state is higher than the lubricated punches.

Now, to have a closer look on how the punches 1 to 4 really differentiate from each other and quantify if the lubricants do have a significant influence in the force signal behavior, the power spectral density of each stroke was calculated for each experiment and plotted in a 3D graph. In the **Figure 5-7**, the evolution of the PSD for every stroke of punch 1 can be seen.

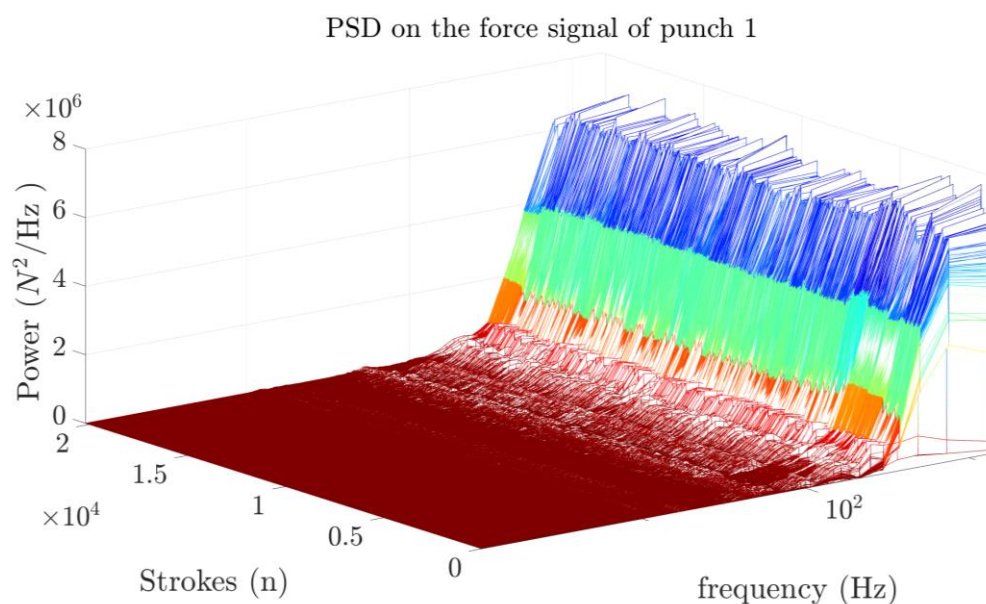


**Figure 5-7** PSD evolution along each stroke

The PSD will allow finding the spectral energy distribution per unit time and its summation or integration along the frequency range yield to the total power contained in the signal. Thus, for every PSD its integral was calculated and then plotted for every stroke. In **Figure 5-8** the scatter plot of these spectral energies distributions can be seen, subsequently from these results a GPR was again performed to evaluate its behavior. The power evolution regressions are shown in **Figure 5-9**.

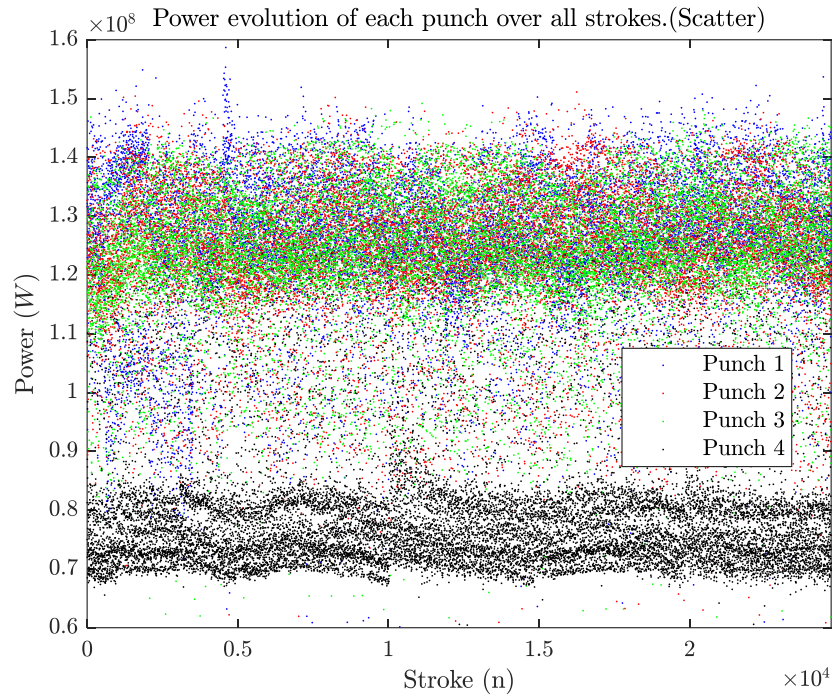


Figure 5-8 Power evolution of the force signal (Scatter plot).

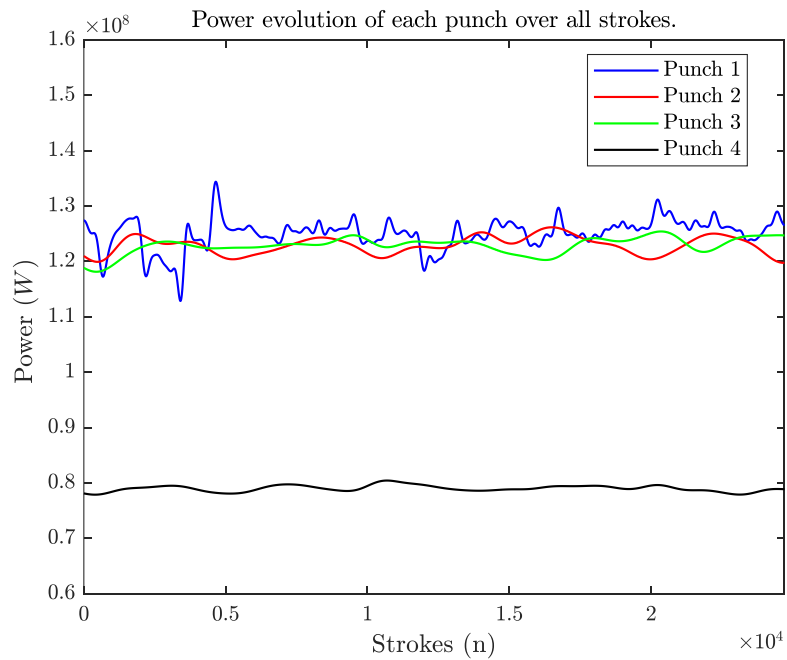


Figure 5-9 Power evolution of the force signal (GPR tendency lines).

From the previous plot, (Figure 5-9), the power behavior fluctuates within the same range for the punches 1 to 3 and an increasing or decreasing observation of these curves can not be deducted. Therefore, in the Figure 5-10, a linear fitting from these curves was then obtained and its results can be seen in Table 5-2.

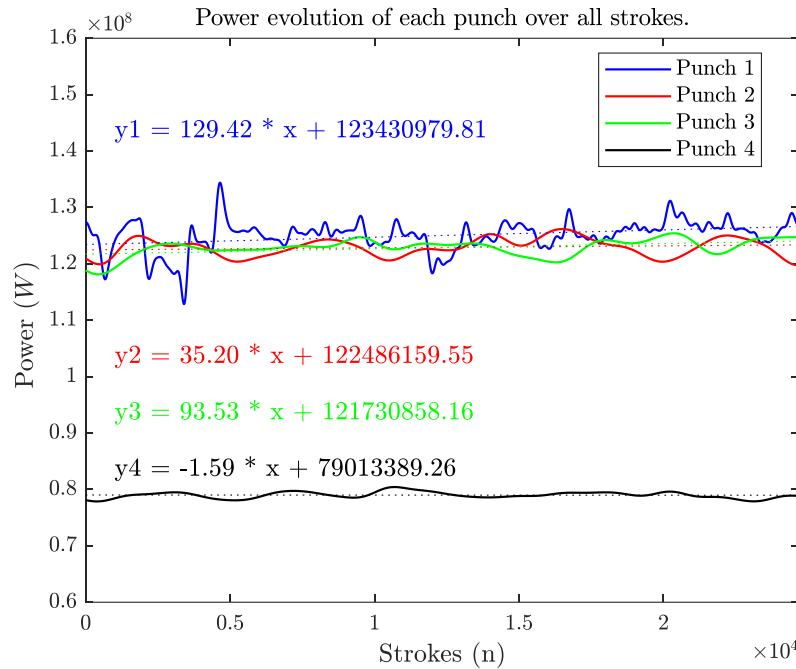


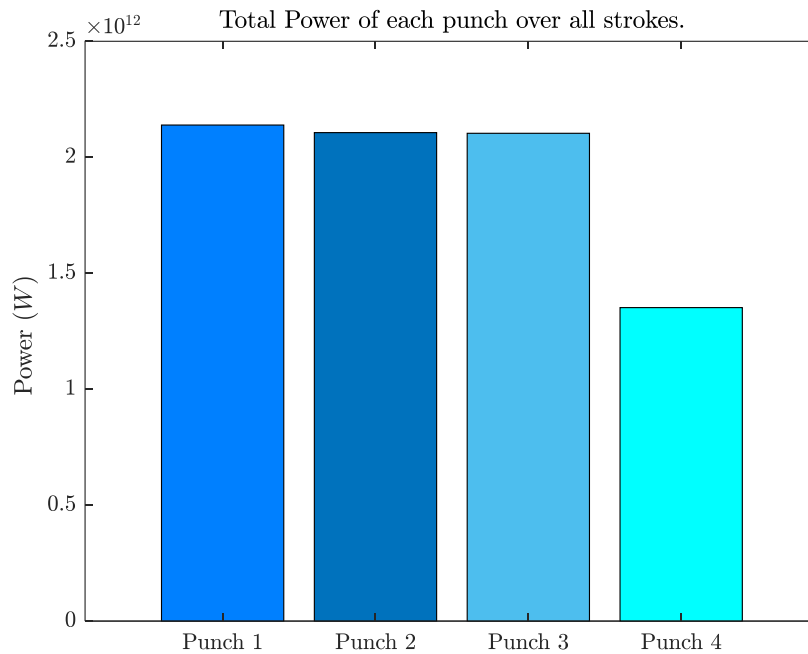
Figure 5-10 Power evolution of the force signal (Linear fitting).

Table 5-2 PSD evolution. GPR and linear fitting results and comparison

Total Power difference	Slope (W/stroke)	Fraction	Diff
Punch 1	129.42	-	-
Punch 2	35.20	1/4	-73%
Punch 3	93.53	5/7	-28%
Punch 4	-1.59	-	-

The previous figure and table showed more clearly and simply how the signal power develops within each stroke of the experiment and whether the trend is actually increasing or decreasing. For punch 1 to 3, it is important to notice and increment tendency of the power and the rate of increment of the power is 73% lower for the punch 2 and 28% lower for punch 3 compared with punch 1 which it the one without lubricant. In this sense, it is now visible an actual effect of the lubricant in the force signal, translated in the power content of it. For punch number 4, the slight negative value of the slope could indicate the system settling into a stable state where less energy is required as the number of strokes increases. In Figure 5-8, for instance for punch 4, it can be clearly seen the set division in along the graph, these divisions could resembles the temperature change of the tool and material while it reaches a steady state, thus for low temperatures, more energy is needed at every stroke. Additionally, the change of metal sheets and the time

between sets, while other measurements were carried on, could also be a reason of these temperatures changes. The PSD represents the variability of the process and the decrement suggest a more consistent process, despite the punch 4 having a smaller side dimension. Additionally, to evaluate the total energy of the whole process, each individual point of **Figure 5-8** was summed and the results are showed in **Figure 5-11** and **Table 5-3**.



**Figure 5-11** Total power contained in every force signal.

**Table 5-3** Total power results and comparison

Total Power difference	Power (W)	Diff
Punch 1	2.11E+12	-
Punch 2	2.08E+12	-1.5%
Punch 3	2.08E+12	-1.6%
Punch 4	1.34E+12	-36.7%

From the previous **Figure 5-11** and **Table 5-3**, it is visible the total power required for every experiment. For the punches 2 and 3, it can be seen a reduction influenced by the usage of lubricant. The punch 3, showed greater reduction of energy with a 1.6% but while punch 2 slightly below this value with 1.5% but as seen previously by the regression results, it is expected to have even more reduction in its behavior since the increment is more than 2 times lower than the one in punch 3. It is important to mention that for bigger number of strokes, these differences will increase in comparison with the dry punch. For punch 4, the difference was -36.7% lower, which means that lower side dimension lead to smaller force requirement.

Interesting is to mention that the punch 4 showed a slight slope decrement, which means that the wear at the punch is increasing by making the cross section area smaller and thus reducing the power requirement.

In various applications, monitoring the PSD of signals from machinery and equipment can help detect faults, wear, or anomalies in their operation. Deviations from the expected PSD can indicate changes in the system's behavior, inconsistencies in the material, tool wear or changing in the cutting conditions. This monitoring could also lead to desired parameters for quality management. For instance, PSD also provides necessary information to minimize unwanted vibrations and improve efficiency by adjusting process parameters. Vibrations are also related to energy efficiency, if the unwanted vibrations are minimized the energy can be transmitted more into forming than into the machinery, thus, improving the lifespan of the equipment's.

## 5.2. Impulse evolution

The results obtained by analyzing the impulse evolution of the force signals over time of every stroke and for every punch can be seen in **Figure 5-12** represented in a scatter plot. In the **Figure 5-13** the GPR tendency lines with its linear regressions of the previous scatter plots are also shown.

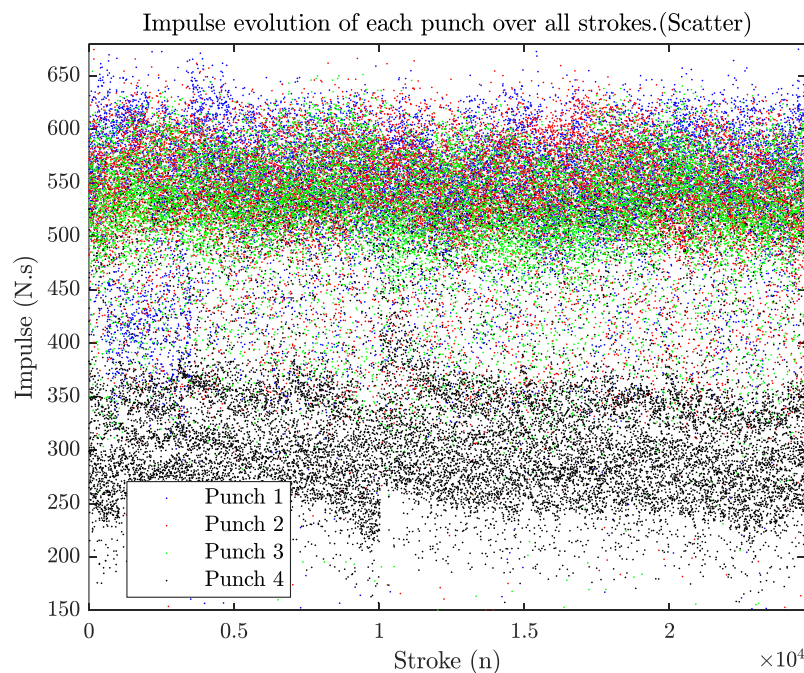


**Figure 5-12** Impulse evolution of the force signal (Scatter plot)

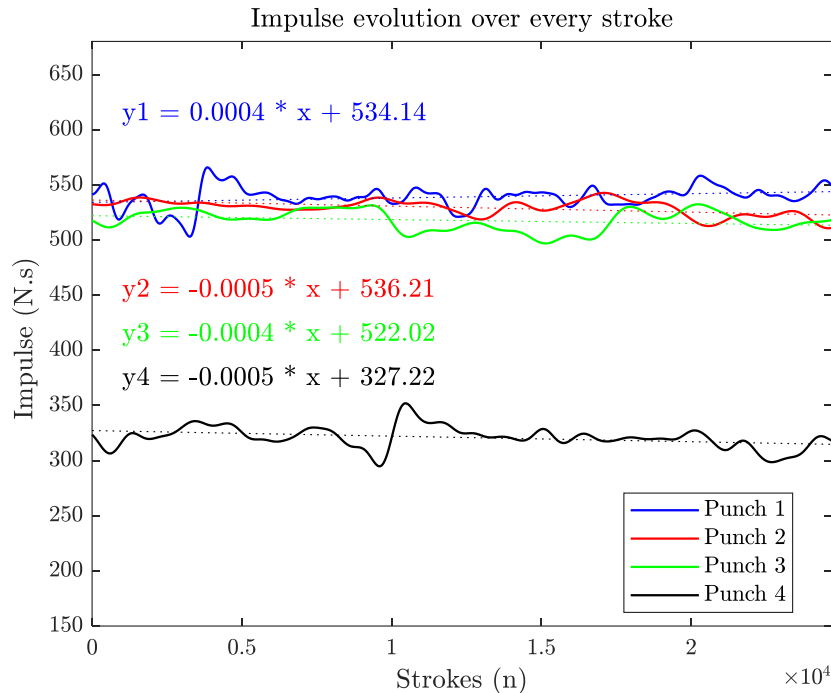


**Figure 5-13** Impulse evolution of the force signal (GPR and linear fitting)

The results showed that for punch 1 to 3, the impulse also lay within the same range of values and for punch 1 the overall tendency is to increase. For the rest of the punches, the tendency is for the impulse to decay slowly, which would indicate that less force is needed in each punch (see **Table 5-4**). The starting point of the impulses of punch 3 is also slightly lower than for the punch 1 and around the number of stroke 5000 the regression of the punch 2 lay under the one of punch 1, which also indicates a positive influence in the desired results of the lubricants.

**Table 5-4** Impulse evolution. GPR and linear fitting results and comparison

Total Impulse difference	Increment / Decrement	Starting point (N.s)	Fraction	Diff
Punch 1	0.04%	534.14	-	-
Punch 2	-0.05%	536.21	1.004	0.39%
Punch 3	-0.04%	522.02	0.977	-2.26%
Punch 4	-0.05%	327.22	0.613	-39.64%

The decrement of the impulse also means the wear of the tool is actually affecting the process, by slightly deforming and incrementing the friction of the tool, the cross section of the punch will decrease by means of material loss. In case of punch 1, build up material at the surfaces of the punch could explain the slight increment of the impulse by means of increasing area. This can also be explained by the equation 2.1 previously mentioned. Similarly, as done before, the total accumulated impulse of the whole process for each punch was then calculated and can be seen **Figure 5-14** and **Table 5-5**. For a greater number of strokes, this decreasing trend is also expected to continue.

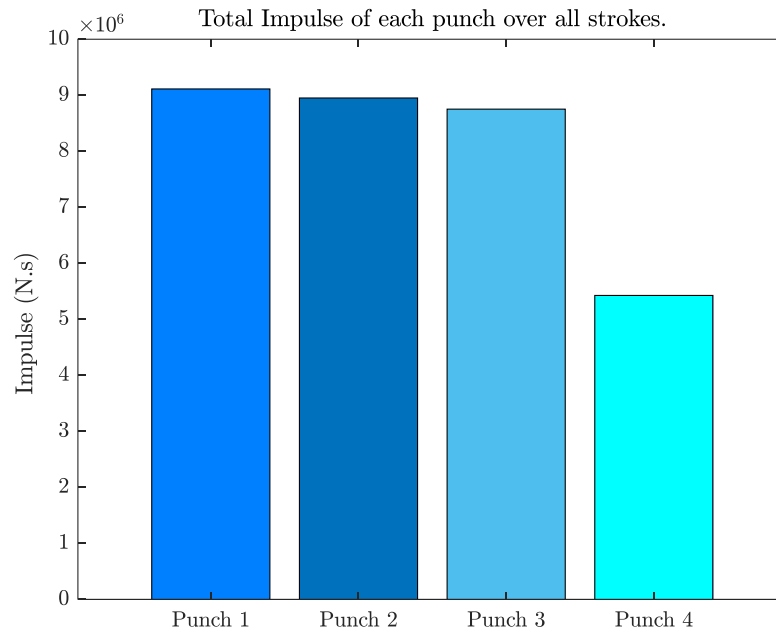


**Figure 5-14** Total impulse contained in every force signal.

**Table 5-5** Total impulse results and comparison

Total Impulse difference	Impulse (N.s)	Diff
Punch 1	9.11E+06	-
Punch 2	8.95E+06	-1.8%
Punch 3	8.75E+06	-4.0%
Punch 4	5.43E+06	-40.4%

The total impulse needed to reach the number of strokes was overall lower for the punches with lubrication. In case of punch 2 and 3 the difference with respect to 1 was of 1.8% and 4 % respectively as seen in **Table 5-5**. By converging the previous results, the PSD and Impulse, regarding the punch 2 and 3 and its trends behaviors it is important to notice that as the blanking process progresses, the initial force applied may be relatively high, resulting in a larger impulse and power (which explains the behavior of some high results at the beginning of every set, see **Figure 5-8** and **Figure 5-12**). Nevertheless, as the number of strokes increases, the system may experience factors such as friction, material deformation, or damping effects that lead to a decrease in the force and, consequently, a decrease in the impulse. Meanwhile, the power may continue to increase due to factors like accumulated energy or the system's response becoming more pronounced.

The increment in the power signal and decrement in the impulse suggest an initial rapid energy transference but as the set continues the force applied results controlled and attenuated, decreasing the impulse. This can be another reason why the initiation and finalization of each set is very noticeable and clearly seen in the

impulse scatter plot (**Figure 5-12**), for instance for punch 4. The number of strokes per set is also a desyncing factor within the experiments.

For a better understating of these force signals, let evaluate the wear development of the tool and how correlates with the quality of the workpiece.

### 5.3. Tool wear

#### 5.3.1. Edge radius wear evolution

The results obtained after measuring each side of the punch and averaging its radii, in each interval corresponding to every experiment, can be seen in the **Table 5-6**. These results were plotted and used to obtain the GPR and linear regressions according to **Figure 5-15**.

**Table 5-6** Edge radius measurements.

	Str.	0	988	2964	4940	9880	14820	19760	24700
<b>Punch 1</b>	r (µm)	25.05	28.98	30.02	28.13	35.93	35.56	41.22	34.90
<b>Punch 2</b>		26.05	29.70	25.20	24.00	27.26	30.74	40.03	41.78
<b>Punch 3</b>		23.94	27.03	27.01	27.77	27.06	29.61	31.78	31.34
<b>Punch 4</b>		21.37	24.36	23.19	26.88	30.53	30.23	33.57	37.66
<b>Std. σ</b>		2.02	/	/	/	/	/	/	/

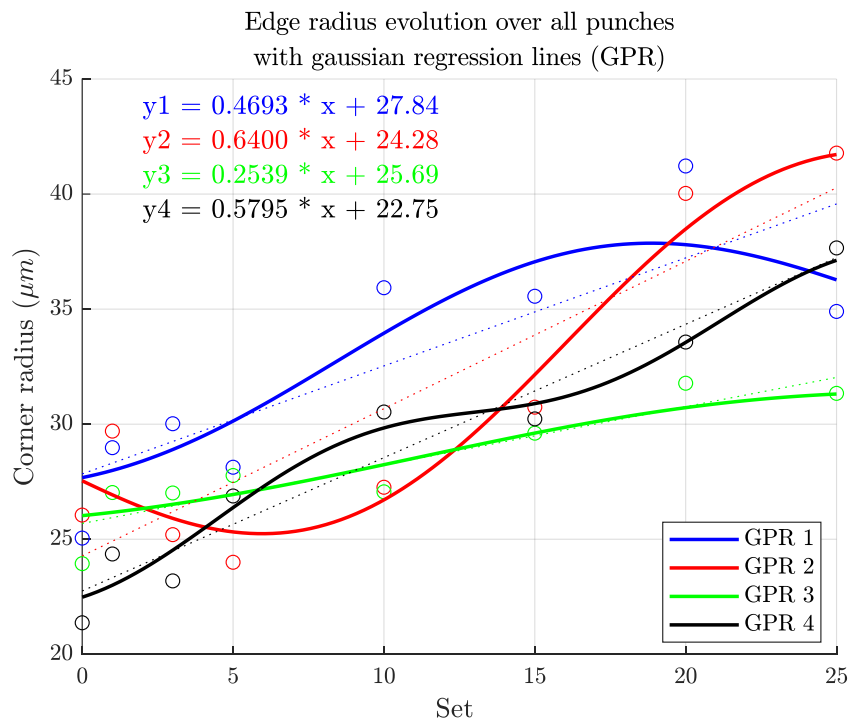


**Figure 5-15** Edge radius evolution

In the previous graph, the evolution of the entire edge radius tends to increase, this means that the tools are losing its sharpness after every set of experiment. It is easy to notice that for every punch, the initial edge radius is different; this is due to the quality tolerance provided by the manufacturer. Nevertheless, the standard deviation of these initial values is small, with a value 2  $\mu\text{m}$ .

**Table 5-7** Edge radius. GPR and linear fitting results and comparison

Edge radius	Slope ( $\mu\text{m}/\text{stroke}$ )	Diff
Punch 1	0.4693	-
Punch 2	0.6400	36.37%
Punch 3	0.2539	-45.90%
Punch 4	0.5795	23.48%

For punch 1, the wear at the edge radius is greater for most part of the experiment in comparison with the other punches with lubricants, this is due to the abrasion and adhesion that occurs also at the edge of the tool that produces built up material that can affect the sharpness. It is interesting to notice that, even though punch 4 has a side length smaller than the others do, the wear evolution can also be visible due to the larger clearance, causes an increased load on the cutting edge similar to the unlubricated punch. For the remaining punches 2 and 3, the lubricants used had a meaningful good influence in this evolution, with punch 3 having the lowest edge radius increment with a -45.90% smaller slope and punch 2 the highest when compared GPR and linear regression with a 36.37% higher slope than the unlubricated. Since these regressions may vary with more data points between each set for a better fitting to train the models, future predictions may lead to an increment of error and thus false estimations.

Since the chemical properties of the lubricants are unknown, it could be deduced that in the case of punches 2 and 4, the influence on the edge is abrasive by increasing the value of the edge radius, but let us evaluate these wear effects in other areas of the tool, such as the side surfaces of the punch and its roughness evolution.

### 5.3.2. Roughness depth Rz evolution at punch surfaces.

The results obtained after measuring each punch side and averaging the roughness lines over each side, as an indicator of tool wear, in each interval corresponding to every experiment, can be seen in the **Table 5-8**. These average results were later used to study the roughness evolution of the punch surfaces along the sets by means of its respective GPR tendency lines (see **Figure 5-16**).

Table 5-8 Roughness depth Rz evolution.

Punch 1	Str.	0	988	2964	4940	9880	14820	19760	24700
	1	5.40	8.20	8.50	8.60	9.50	10.70	11.80	13.20
	2	5.10	7.30	8.20	7.90	8.20	8.30	8.80	9.60
	3	5.10	7.00	7.70	7.30	7.60	6.70	6.90	7.50
	4	4.80	6.40	7.00	6.80	6.90	6.50	6.50	6.90
	5	4.50	5.40	6.40	6.20	6.30	6.00	5.60	5.90
	6	5.10	6.20	7.50	6.70	6.80	6.50	6.20	6.70
	7	5.10	5.60	6.30	5.70	7.20	6.80	6.20	6.90
	8	5.10	5.30	4.70	5.80	7.20	6.00	5.90	7.30
	Av.	5.03	6.43	7.04	6.88	7.46	7.19	7.24	8.00

Punch 2	Str.	0	988	2964	4940	9880	14820	19760	24700
	1	4.70	5.50	6.60	7.60	8.30	8.90	10.20	9.20
	2	4.50	4.70	4.60	5.20	5.10	5.70	6.30	5.90
	3	4.50	4.80	4.70	5.20	4.70	5.20	5.80	5.40
	4	4.40	4.50	4.50	5.00	4.70	5.20	5.50	5.10
	5	4.40	4.30	4.50	4.80	4.30	4.60	4.90	4.50
	6	4.50	4.70	4.70	5.30	5.00	4.70	5.30	5.10
	7	4.10	4.30	4.10	5.00	4.20	4.80	5.40	4.60
	8	4.50	4.40	4.20	4.60	4.20	4.70	4.20	3.90
	Av.	4.45	4.65	4.74	5.34	5.06	5.48	5.95	5.46

Punch 3	Str.	0	988	2964	4940	9880	14820	19760	24700
	1	4.60	6.50	6.70	6.60	7.00	6.40	8.90	7.40
	2	5.10	6.10	5.40	5.90	5.80	5.50	6.20	5.60
	3	4.70	6.00	5.30	5.90	5.70	5.50	5.10	5.20
	4	4.70	6.00	5.20	5.70	5.40	5.40	4.80	4.80
	5	4.90	5.90	5.20	5.80	5.50	5.60	4.60	5.20
	6	5.20	6.50	5.90	6.20	6.10	6.00	5.00	5.70
	7	5.00	6.50	4.70	6.10	4.80	6.10	5.30	4.00
	8	5.20	6.00	4.80	3.90	4.80	4.30	4.80	4.20
	Av.	4.93	6.19	5.40	5.76	5.64	5.60	5.59	5.26

Punch 4	Str.	0	988	2964	4940	9880	14820	19760	24700
	1	4.70	4.60	5.10	5.00	5.90	5.50	6.20	5.60
	2	4.70	4.50	4.80	4.60	5.20	4.60	5.10	4.60
	3	4.40	4.70	4.90	4.50	5.00	4.30	4.70	4.10
	4	4.40	4.70	4.70	4.40	5.10	4.20	4.60	3.90
	5	4.50	4.70	4.90	4.40	5.30	4.30	4.50	4.50
	6	5.20	4.80	5.80	5.00	5.50	4.70	5.10	5.00
	7	4.20	6.00	4.40	4.50	4.70	4.00	4.60	4.00
	8	4.70	5.10	4.90	4.90	4.90	4.60	5.10	4.00
	Av.	4.60	4.89	4.94	4.66	5.20	4.53	4.99	4.46

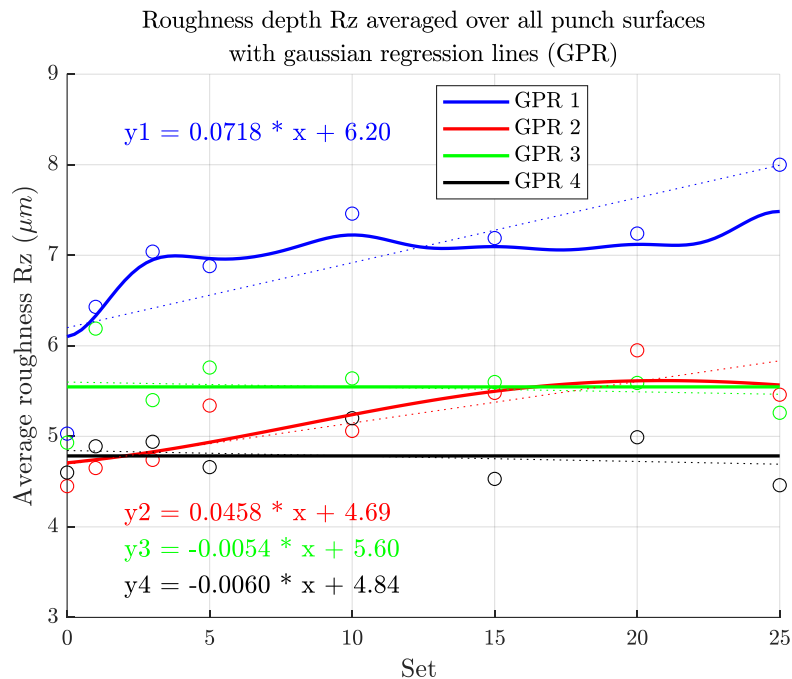


Figure 5-16 Roughness evolution of the punch surfaces. (GPR and Linear regression)

From the previous graph, it is remarkable to notice how the roughness of the punches with lubricants tend to prevail within the initial range values, which indicates a good influence by not incrementing this wear indicator and reducing the friction between the punch and the material and by reducing the temperature and wear compared to the one unlubricated. In Figure 5-16, the initial wear of punch 1 is remarkably higher than the rest of the lubricated punch and this abrasion effect continues along the experiment with a high increasing roughness behavior, seen after performing the regression models. For punch 3 and 4 the averaged roughness tends to slightly decrease with a really low rate while punch 1 and 2 increase.

Table 5-9 Roughness evolution. GPR and linear fitting results and comparison

Roughness Rz	Slope (µm/stroke)	Diff
Punch 1	0.0718	-
Punch 2	0.0458	36.21%
Punch 3	-0.0054	101.15%
Punch 4	-0.0060	101.28%

In Table 5-9, the slope of punch 3 and 4 could be considered as constant since no remarkable roughness increment can be seen, this quasi constant tendency could be explained as the lubricant, over time, spreads and gets distributed more evenly, it can contribute to smoother and more consistent surface finishes, resulting in a decrease in roughness values. The lubricant can also coat micro-level imperfection that can create smoother surface. When a new punch is installed, its surface might have certain micro-level irregularities, or "asperities." During the initial strokes, these asperities may be worn down or smoothed out due to the interaction with the workpiece material [4].

The GPR lines and the linear regression lines for punch 3 and 4 almost match with each other and it indicates a high level of correlation or similarity between the two models. The fact that both the linear regression and Gaussian regression process yield almost identical regression lines suggests a strong correlation between the data points being analyzed. This implies that the relationship between the independent and dependent variables can be effectively captured by both model and provides consistency in the results regardless the modelling approach. For better fitting a modelling in this study case, it is always desired to have more data point with more experiment sets.

## 5.4. Workpiece quality

### 5.4.1. Shear zone roughness evolution

After observing how does the punch wear evolution behave, let us have a look on the behavior of some remarkable aspects in the quality of the workpiece. The results obtained, after having measured the shear zone roughness of the initial and final workpieces corresponding to each set of each experiment and averaging their values, as an indicator of workpiece quality, can be seen in the **Table 5-10**. Furthermore, the GPR and linear regressions of the shear zone roughness evolution can be seen in the **Figure 5-17** and in **Table 5-11**.

**Table 5-10** Average shear zone sample roughness

Set	Punch 1	Punch 2	Punch 3	Punch 4
1	11.98	15.44	12.41	17.11
2	19.43	17.76	14.51	18.74
3	21.48	16.65	14.50	15.92
4	14.86	14.44	19.17	15.91
5	13.17	17.36	13.98	15.81
6	15.23	16.11	13.92	15.27
7	14.40	19.77	14.18	14.09
8	14.26	15.27	14.71	12.88
9	13.90	13.51	15.47	13.76
10	14.77	15.24	13.01	15.78
11	15.75	15.14	14.86	12.70
12	16.17	15.29	18.50	16.82
13	13.24	15.61	14.36	13.81
14	14.10	16.59	13.36	15.47
15	15.50	12.96	13.67	17.98
16	16.39	16.96	17.39	13.77
17	15.77	14.40	17.19	13.51
18	14.79	14.10	15.48	14.09
19	13.26	13.16	13.48	17.39
20	17.50	13.46	13.07	15.57
21	15.09	16.01	14.92	15.07
22	15.10	15.21	13.17	15.13
23	14.99	12.46	16.49	13.52
24	15.70	14.95	12.73	17.71
25	16.09	15.62	15.00	13.98

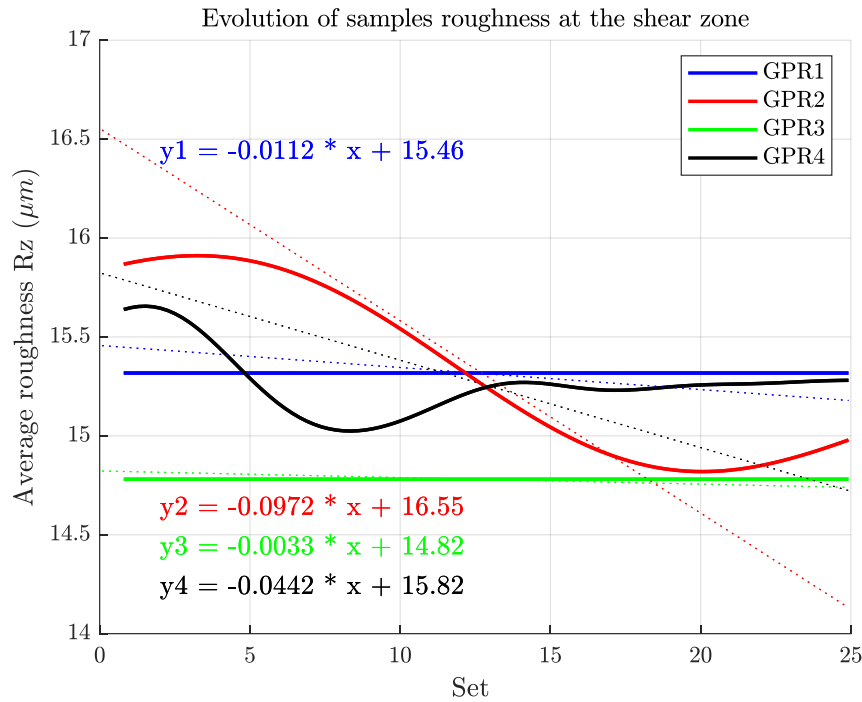


Figure 5-17 Roughness sample evolution (GPR and Linear regressions)

Table 5-11 Shear zone roughness evolution. GPR and linear fitting results and comparison

Shear zone roughness $R_z$	Slope ( $\mu\text{m}/\text{stroke}$ )	Diff	Starting point ( $\mu\text{m}$ )	Diff
Punch 1	-0.0112	-	15.46	-
Punch 2	-0.0972	767.86%	16.55	7.05%
Punch 3	-0.0033	70.54%	14.82	4.14%
Punch 4	-0.0442	294.64%	15.82	2.33%

In this case, the tendency lines showed the best results for punch 2, where a deeper decay in roughness although for every punch the decrement behavior was also followed, with minor differences in its GPR and linear regressions (see **Table 5-11**). For instance, punch 2 has an intense decrement in its behavior but as well with punch 4; tend to stabilize as the number of set increases and so do as well the rest. A decrement tendency in the roughness of the shear zone, suggests that the material is being effectively sheared and the irregularities on the surface are being smoothed out. These results are desirable in blanking operations, as it indicates that the material is being cut cleanly and the process is producing a good finish. For punch 3, the results showed the lowest roughness of all and with a low decay tendency, this also relates to the previous graph since this tool experienced the lowest edge radius wear.

### 5.4.2. Cross section evolution

Now, let us evaluate each section evolution of the workpieces according to **Figure 2-5**. The cross-section evolution of the samples related to every punch can be seen in the **Figure 5-18**.

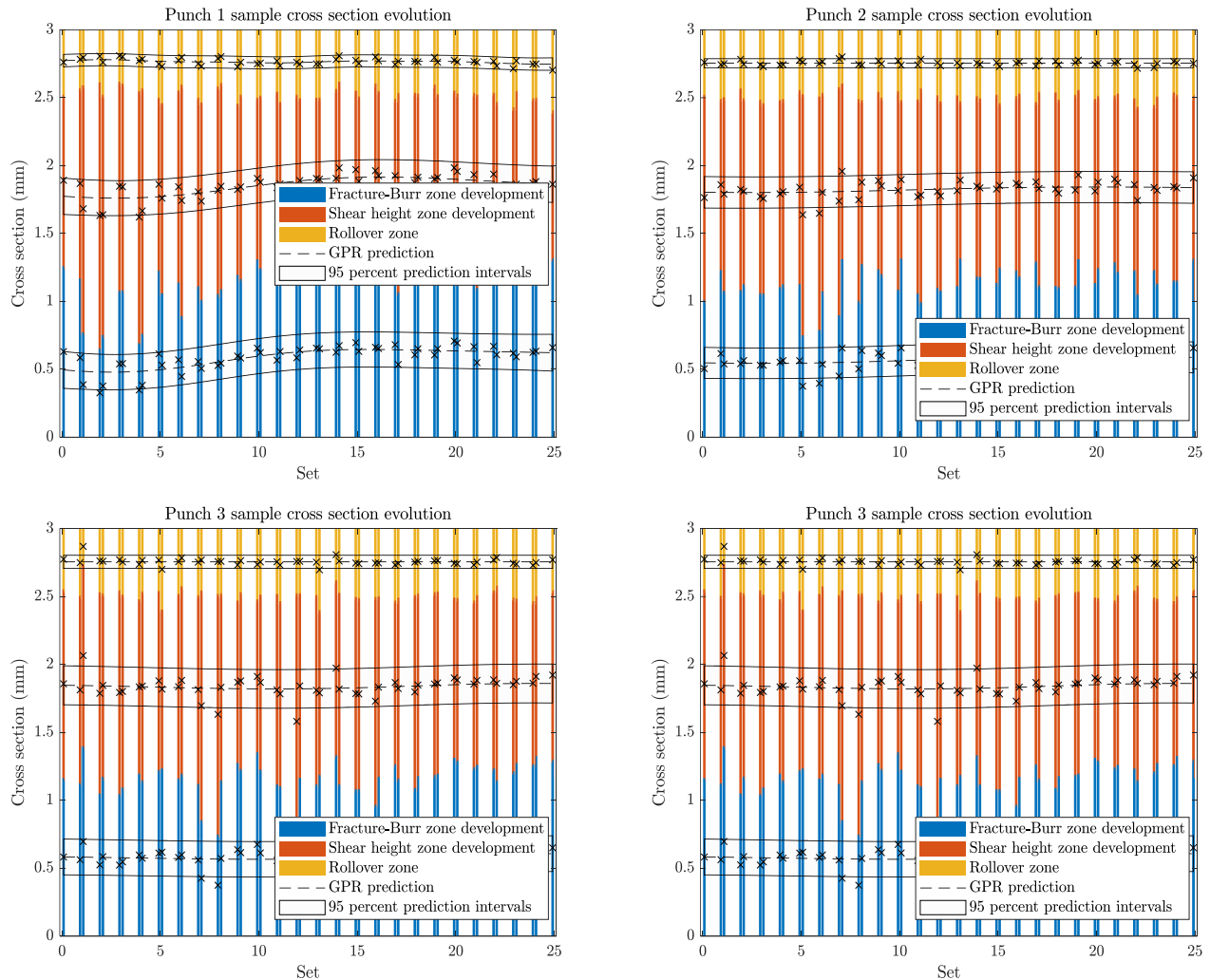


**Figure 5-18** Sample cross-section evolution for every experiment.

The evolution of each section within the workpiece can be seen in the previous graph. The Bar plot resembles each section of the blanking process and the GPR lines with the prediction intervals, the regression of these results. The “x” markers represents the measurements obtained (see **Appendix C**) and the dotted line the GPR by means of 100 testing samples after the model was trained so the 95% prediction intervals can be obtained. Interesting to notice how the prediction intervals contains more likely, the largest amount of data points and resembles the range in which the values could land.

The shear zones heights of the workpieces of punch 2 and 3 depicted in the graph showed a quasi-stable behavior, where each limit of these values provided low variance. For punch 1, the shear zone height tends to stabilize after 10 sets but tend to decrease after set 16. This decrement could be caused by factors such as work hardening, heat accumulation, or relaxation of internal stresses as the material becomes more resistant to deformation since this punch is unlubricated.

It is notable, that shear zone height of the workpieces from punch 4 have the lowest desirable values among the others, this is due to the fact of the smaller tool side dimensions and where the effect of this higher clearance between die and punch does has a negative effect in this study. It shows a very high rollover and fracture-burr zone heights with decrement at the shear zone.

### 5.5. Ranking and comparison

The results of the ponderation are given in **Table 5-12**, additionally for some of the evaluations, the same value was given to the results that were likely to be similar or showed the same trend or behavior as mentioned before.

**Table 5-12** Ponderation and grading results.

	Parameter	Val	Punch 1	Punch 2	Punch 3	Punch 4
Force	Power evolution.	2	4	2	3	1
	Impulse evolution.	2	4	2	2	1
Tool wear	Edge radius evo.	2	3	4	1	2
	Roughness surface evo.	1	4	2	3	1
Workpiece	Rollover	1	3	2	1	4
	Burnish	3	3	1	1	4
	Fracture-Burr zone	1	2	1	2	4
	Roughness evo.	2	2	1	2	4
<b>Result</b>			<b>3</b>	<b>2</b>	<b>2</b>	<b>3</b>

The previous tables depicted the summary of all of the results obtained within this investigation. Regarding the parameter considered for the workpiece section, it is clear to notice that the punch 2 got the overall best results, followed by punch 3. The most remarkable results that can be addressed is how the lubrication affected the roughness of the shear zone in the workpiece, by reducing it considerable according to **Figure 5-17**.

On the other hand, considering the tool wear and the force applied, punch 3 got the best evaluation among the others and as expected the lack of lubrication in punch 1 showed the highest values regarding force evolution. Punch 4 results demonstrated, that not only having a smaller side dimension could lead to smaller blanking forces but also can lead to considerable lower tool wear evolution.

Even though punch 2 and punch 3 showed similar results after the evaluation for each of the parameters considered it is important to notice that for punch 2, the quality of the workpiece was better than for punch 3. The aim of every manufacturing process is to obtain a high-quality end product and considering the

similar results for the force and tool wear value, the lubricant FN 6870-38 used in punch 2 is the overall selection to be made.

## 6. Future experimental considerations

In the aftermath of this project, some considerations can be achievable in order to optimize the experiments and the data acquisition to depict deeper fields of studies and convergence of results. Some of these recommendations are listed below:

- *Production cost:* For each of the lubricants, the cost, availability and carbon foot print were not considered. The post processing costs, depending on the type of manufacturing process that is it being carried out, was also not considered. But since the usage of lubrication does not represent high cost in comparison of the workpiece is it remarkable to notice the other factors for a better decision making.
- *Tooling parameters:* can be adjusted within each stroke in order to optimize the cutting conditions, such as cutting speed, lubrication rate and tool geometry, but since in this case these parameters were fixed the aim was to address the exact procedure for each of the experiment.
- *Material properties and tool shape:* a thinner and more ductile material could lead to more shearing, less tool wear and less force applied and thus post processing can be reduced. This study was held for specific conditions in tooling, material and workpiece geometry in order to visualize this result in a clearer way.
- *Additional measuring tools:* The usage of accelerometer could provide a better understanding of the vibrations of the machine and how can it later be mitigated in order to decrease the wear of the tool and increase the quality of the product due to unnecessary vibrations. The use of thermocouple, can help to study the temperature development during the process which affects the tribological load on the system and also decompose the lubricant additives.
- *Sampling:* The reproducibility of these experiments is as well something to considered. Only one punch was used for each of these experiments. More set of experiments for any specific lubricant, would provide more reliable results concerning tool wear evolution and variance in results. For the quality of the workpiece, each sample was related to a specific stroke and not a group of samples to the same stroke, thus more accurate and narrower confidence intervals can be obtained.
- *Number of strokes:* In these manufacturing processes, the number of strokes carried by the machine are considerable higher. For higher number of strokes, it is expected to be showed higher differences in the quality of the workpiece, tool wear evolution, force signals and prediction intervals among each experiment. But, to carry out this point, higher investments should be made or to implement into an ongoing production line. For higher number of strokes, the appearance of new amplitudes at lower frequencies could be an important factor to consider in predicted maintenance.
- *Machine learning models:* Even though only one method was implemented for GPR by means of Kernel functions and square exponential, for lubrications with similar properties, these preliminary results could be useful to train other models to obtain preliminary simulation results and better fitting. But this could only be applicable for the same tool shape.

- *Tool wear*: The most remarkable wear in the tool is the edge radius since the abrasion couldn't be measured because of the adhesion of the buildup material while blanking. Other effects such as crater wear, corner chipping and cracks were not highly visible due to the low number of strokes and time expended to perform each complete experiment. More ambient conditions could affect the tool wear, since production could take weeks before tool replacements.
- *Workpiece quality*: A criteria to certify if the quality of the workpiece fulfills the production requirements in a production line of a desired company at certain number of strokes, was not given. Depending of the usage and application of the workpiece that is it being produced, the functionally could be preserved despite some loses in the esthetics.
- *Maintenance*: the force effects, despite its analysis and if it really have a major effect in the machine and its maintenance, were not covered by this study. Some machine modifications can be implemented to address some maintenance and operability problems that could reduce the overall cost of the process.
- *Quality parameters*: The manufacturer could stablish a range interval in the force signal after a certain number of strokes in order to link the previous results obtained related to tool wear and product quality. The aim is to only measure the force signal and gather its amplitude and frequency decomposition by means of the FFT, PSD and impulse. This could save time and cost, due to unnecessary production line stops.

## 7. Conclusions

After performing the previous studies, it can be concluded that:

- The study of the force signal evolution in the blanking manufacturing process for different type of lubrications with a square punch was carried out.
- The FFT and PSD decomposition of the force signals was performed and the total power contained in the signal was obtained, resulting in a considerable energy reduction due to the lubrication. For punch 2 and 3 the results showed were similar with reduction of 1.5% and 1.6 % respectively. Due to a lower side dimension, punch 4 also depicted how the geometry could affect the force signal. These really small difference could be a results of data acquisition and longer number of strokes could clear out this problem, but the tendency of each of the regressions showed lower increment ratios compared with punch 1, with a reduction of 73% and 28% respectively.
- The Impulse calculation demonstrated the correlation between the force signal and the wear of the tool. It resulted as a great indicator of how to determine the decrement of the force per stroke and how its behavior per set is related to factors such as frictions, damping effects and material deformation. For punch 2 and 3 the results showed were similar with a reduction of 7.3 % and 8.6% respectively with respect to the unlubricated one and a decrement tendency of 0.05% and 0.04% per stroke. For punch 4, this decrement was higher due to the smaller dimension with a reduction of 40.2%. The tendency followed by the GPR and linear regression of the lubricated punches tended to decrease, thus it can be concluded that less build up material formed at the surface of the punches.
- The tool wear was studied considering the edge radius and the roughness at the surface of the punch and its tendency behavior among every stroke of the experiment. Despite lubrication, some punches experienced a higher edge radius increment that the one unlubricated, being punch 2 the one with the greater value. The greater clearance in punch 4, resulted in lower forces and also low tool wear, for instance at the edge radius evolution.
- The roughness evolution at the surface of the punch was also considered as a wear factor due to the adhesion and abrasion happening simultaneously while blanking. The usage of lubrication enhanced the overall roughness of the punches by having lower values with respect of the unlubricated punch.
- The cross-section evolution study of the samples depicted how lubrication enhanced the consistency of the shear zone height and how a lower side radius of the punch could lead to increment of the rollover and fracture zone (for the case of punch 4). The samples from punch 2 and 3 showed similar trend behavior with narrower prediction intervals compared to the unlubricated punch, i.e., better quality.
- The roughness evolution at the shear zone of the samples was analyzed as a quality factor to proof the cut. The results indicated, that the punch 3 got the best results which could indicate lower friction at the cutting surfaces, followed by punch 2.
- A ponderation was stablished in order to evaluate each of the previous results and to select the best lubrication for the process. The ponderation showed that the experiments related to punch 2, obtained the best workpiece quality while on the other hand, punch 3 obtained the best results in terms of tool wear and force signal evolution. Since these two experiments (2 and 3) showed similar

results, for these numbers of strokes, the difference between them was not significantly high. Acknowledging that other factors could influence the lubrication selection such as cost, carbon foot-print and availability, which were not considered, and that the product quality is the most desirable factor in a manufacturing process, the best lubrication resulted in to be FN 6870-38, related to punch 2.

- Future experimental considerations were addressed in order to obtain more reproducible results and improve the test mechanism for deeper study analysis and further training for different regression methods in order to reduce the variance in the results.

## 8. Bibliography

- [1] G. Schuler, *Metal Forming Handbook*, Springer, 1998.
- [2] A. T. Taylan Altan, *Sheet Metal Forming. Process and Applications*, Ohio 44073-002: The Materials Information Society. ASM International, 2012.
- [3] B.-A. B. Eckart Doege, *Handbuch Umformtechnik: Grundlagen, Technologien, Maschinen*, Leibniz Universität Hannover.: Springer-Verlag Berlin Heidelberg, 2010.
- [4] M. P. M. A. D. M. Moghadam, "Analysis of lubricant performance in punching and blanking," *Tribology International*, vol. 141, 2020.
- [5] S. G. a. F. M. Johnson, "A Modified Split-Radix FFT With Fewer Arithmetic Operations," *IEEE Transactions on Signal Processing*, vol. 55, pp. 111-119, 2007.
- [6] "Fast Fourier Transformation FFT - Basics," NTI Audio, 12 07 2023. [Online]. Available: <https://www.nti-audio.com/en/support/know-how/fast-fourier-transform-fft>.
- [7] S. Hanly, "Vibration Analysis: FFT, PSD, and Spectrogram Basics," ENDAQBLOG, [Online]. Available: <https://blog.endaq.com/vibration-analysis-fft-psd-and-spectrogram>. [Accessed 11 07 2023].
- [8] TRUMPF, "Punching Machines TruPunch 5000," TRUMPF SE und Co. KG , 12 07 2023. [Online]. Available: [https://www.trumpf.com/en\\_US/products/machines-systems/punching-machines/trupunch-5000/](https://www.trumpf.com/en_US/products/machines-systems/punching-machines/trupunch-5000/).
- [9] Keyence Deutschland GmbH, "Optische Messmaschine LM," [Online]. Available: [https://www.keyence.de/landing/lpc/optische\\_messmaschine.jsp?aw=google\\_KD\\_BR\\_QMS06&SL=05&gad=1&gclid=Cj0KCQjw1rqkBhCTARIsAAHz7K2g\\_d6v5L-\\_k1vG7eEuis\\_hdVm8th09QD\\_rOpQGgOVRsR2nalPb6PkaAnifEALw\\_wcB](https://www.keyence.de/landing/lpc/optische_messmaschine.jsp?aw=google_KD_BR_QMS06&SL=05&gad=1&gclid=Cj0KCQjw1rqkBhCTARIsAAHz7K2g_d6v5L-_k1vG7eEuis_hdVm8th09QD_rOpQGgOVRsR2nalPb6PkaAnifEALw_wcB). [Accessed 10 07 2023].
- [10] P. P. A. E. V. R. K. P. Lind L, "Description of punch wear mechanism," *Proceedings of 7th International Conference of DAAAM*, pp. 504 - 509, 2010.
- [11] B. N. A. J. Olsson DD, "Lubricant test for punching and blanking," *JSTP Journal*, vol. 44, p. 50, 2003.
- [12] B. N. A. J. Olsson DD, "Studies of lubricants and punch design in punching of stainless steel," *Proceed. of Int. Conf. on Recent Advances in Manufacture & Use of Tools & Dies and Stamping of Steel Sheet*, pp. 123-137, 2004.

- [13] B. N. A. J. Olsson DD, "Analysis of Pick-Up Development in Punching," *CIRP*, vol. 51, pp. 185-90, 2002.
- [14] B. F. O. d. H. M. Schmidt RA, "Tribologie beim Scherschneiden und Feinschneiden.," vol. 52, pp. 42-54, 2005.
- [15] S. Brown., *Machine learning, explained*, Massachusetts: Management Sloan School, Massachusetts Institute of Technology, 2021.
- [16] Berkeley, School of Information, "What is Machine Learning (ML)," UC Berkeley School of Information, [Online]. Available: <https://ischoolonline.berkeley.edu/blog/what-is-machine-learning/>. [Accessed 11 01 2023].
- [17] C. W. C.E. Rasmussen, *Gaussian Processes for Machine Learning*, MIT Press, 2006.
- [18] "DC04 | 1.0338," Thyssenkrupp Materials Processing Europe GmbH, [Online]. Available: <https://www.thyssenkrupp-materials-processing-europe.com/en/c-steel/cold-rolled-sheet/dco1-dc07/dc04>. [Accessed 12 07 2023].
- [19] Trumpf, "TruServices Stanzwerkzeuge," [Online]. Available: [https://www.trumpf.com/filestorage/TRUMPF\\_Master/Products/Services/01\\_brochures/TRUMPF-punching-tools-catalog-DE.pdf](https://www.trumpf.com/filestorage/TRUMPF_Master/Products/Services/01_brochures/TRUMPF-punching-tools-catalog-DE.pdf). [Accessed 11 07 2023].
- [20] B. Adero, "Experimental investigations of mechanical anisotropy of Freiberg gneiss.," Ruhr-Universität Bochum, Institute of Geology, Mineralogy and Geophysics, Bochum, 2020.
- [21] E. Zio, *The Monte Carlo Simulation Method for System Reliability and Risk Analysis*, London: Springer, 2013.
- [22] W.-L. J. Yong Bai, "Basics of Structural Reliability," in *Marine Structural Design*, London, Elsevier Ltd. All rights reserved., 2015, pp. 581-602.
- [23] The MathWorks, Inc., "MATLAB Math. Graphics. Programming.," The MathWorks, Inc., 2022. [Online]. Available: <https://www.mathworks.com/products/matlab.html>. [Accessed 18 9 2022].
- [24] F. H. & V. B. Cornet, "In situ stress determination from hydraulic injection test data," *Journal of Geophysical Research*, vol. 89, no. <https://doi.org/10.1029/JB089iB13p11527>, pp. 11527-11537, 1984.
- [25] M. D. Zoback, "Reservoir Geomechanics. Cambridge University Press," Cambridge University Press., Cambridge., 2010.
- [26] R. M. S. M. Ronald Walpole, *Probability and Statistics for Engineering and the Sciences*, Virginia : Pearson, 2012.

- [27] X. Z. Z. Qide Zheng, "State-of-the-art and future challenge in fine-blanking technology," *Production Engineering*, vol. Springer, no. <https://doi.org/10.1007/s11740-018-0839-7>, pp. 61-70, 2018.

## 9. Appendix

### 9.1. Appendix A

#### Sample holder

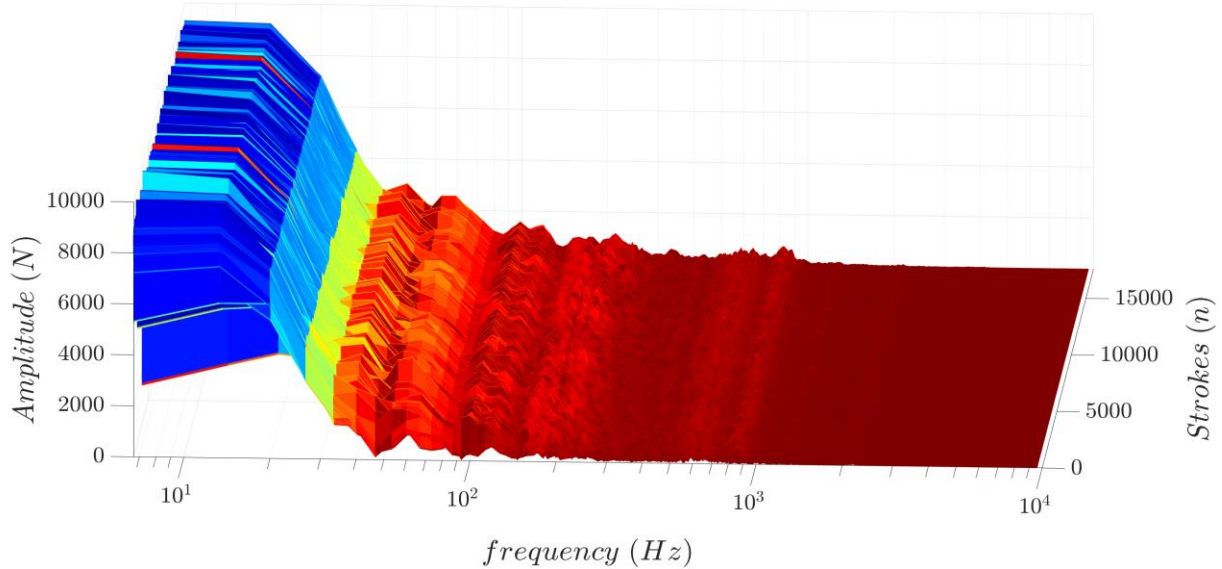


**Appendix A- 1** Sample holder used in the profilometer

## 9.2. Appendix B

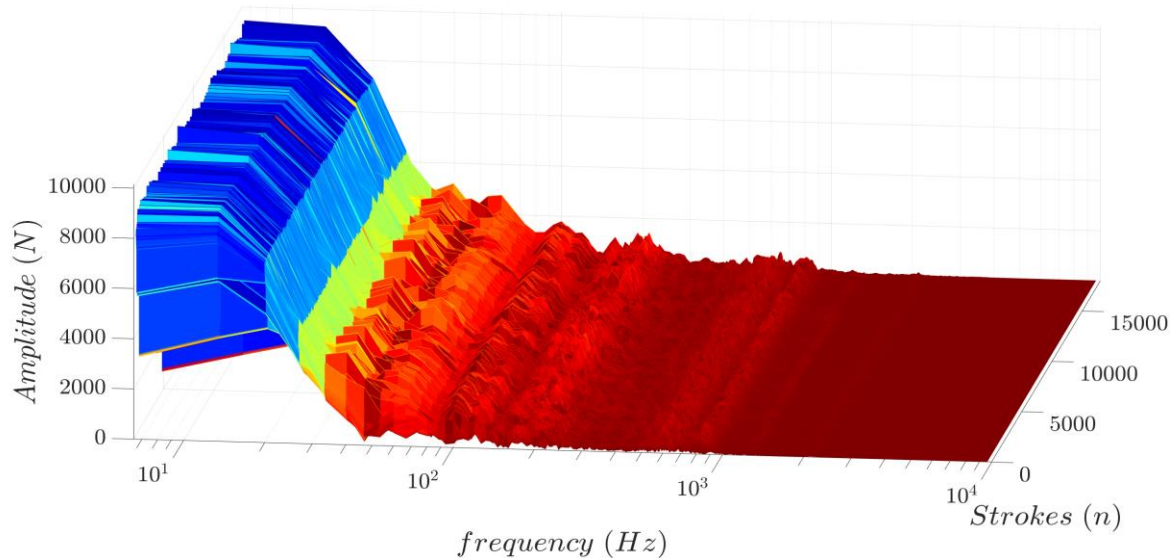
### FFT signal evolution

FFT on the force signal of punch 2

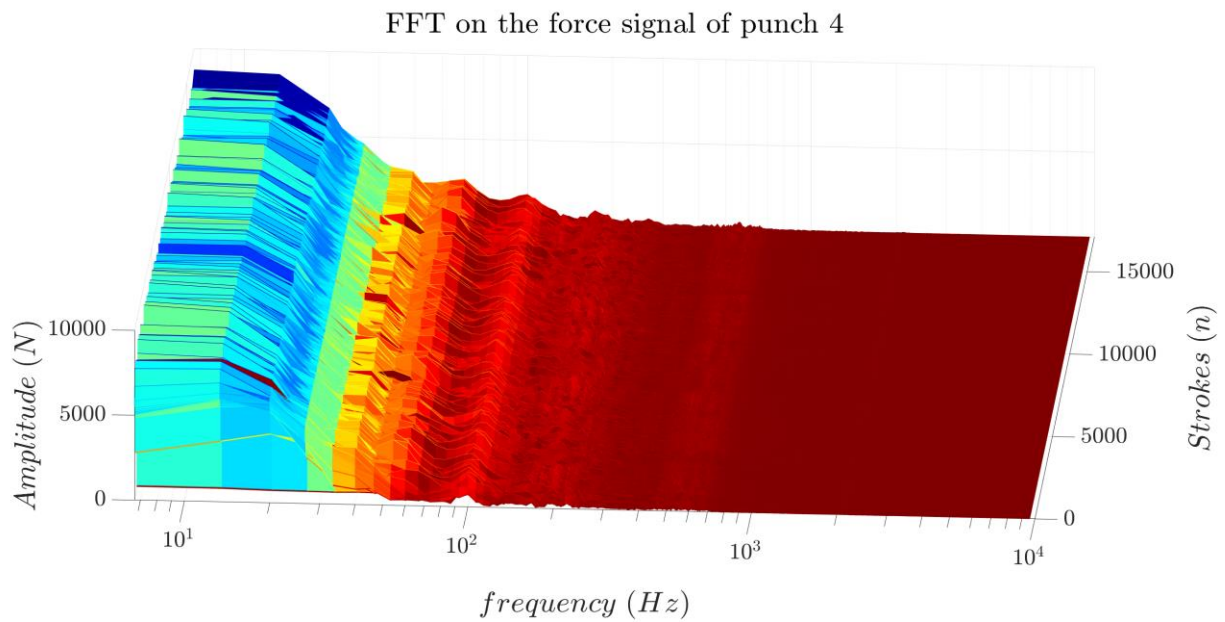


**Appendix B- 1** FFT evolution along each stroke. Punch 2

FFT on the force signal of punch 3



**Appendix B- 2** FFT evolution along each stroke. Punch 3



**Appendix B- 3** FFT evolution along each stroke. Punch 4

### 9.3. Appendix C

#### Cross section sample evolution data

Due to high number of data points, only half of the point are shown in the following tables

**Table 9-1** Punch 1. Cross section zones evolution data

Set	Rollover (mm)	Shear zone height (mm)	Fracture-Burr (mm)
1	0.478	1.260	1.262
	0.434	1.394	1.172
3	0.478	1.767	0.755
	0.383	1.537	1.080
5	0.432	1.803	0.765
	0.504	1.267	1.229
7	0.407	1.699	0.894
	0.500	1.386	1.114
9	0.394	1.516	1.090
	0.547	1.258	1.195
11	0.490	1.264	1.246
	0.458	1.408	1.134
13	0.505	1.210	1.285
	0.502	1.185	1.313
15	0.382	1.269	1.349
	0.451	1.156	1.393
17	0.456	1.237	1.307
	0.511	1.126	1.363
19	0.472	1.226	1.302
	0.407	1.382	1.211
21	0.473	1.139	1.388
	0.467	1.199	1.334
23	0.533	1.252	1.215
	0.573	1.189	1.238
25	0.502	1.231	1.267
	0.594	1.086	1.320

**Table 9-2** Punch 2. Cross section zones evolution data

Set	Rollover (mm)	Shear zone height (mm)	Fracture-Burr (mm)
1	0.481	1.509	1.010
	0.513	1.255	1.232
3	0.506	1.365	1.129
	0.517	1.422	1.061
5	0.512	1.360	1.128
	0.445	1.428	1.127
7	0.469	1.456	1.075
	0.423	1.676	0.901
9	0.520	1.204	1.276
	0.458	1.303	1.239
11	0.520	1.165	1.315
	0.516	1.426	1.058
13	0.529	1.390	1.081
	0.485	1.399	1.116
15	0.509	1.310	1.181
	0.482	1.381	1.137
17	0.474	1.340	1.186
	0.533	1.173	1.294
19	0.515	1.377	1.108
	0.482	1.397	1.121
21	0.491	1.262	1.247
	0.487	1.225	1.288
23	0.567	1.379	1.054
	0.556	1.210	1.234
25	0.483	1.363	1.154
	0.496	1.188	1.316

**Table 9-3** Punch 3. Cross section zones evolution data

Set	Rollover (mm)	Shear zone height (mm)	Fracture-Burr (mm)
1	0.449	1.386	1.165
	0.500	1.375	1.125
3	0.479	1.351	1.170
	0.458	1.496	1.046
5	0.466	1.387	1.147
	0.462	1.316	1.222
7	0.429	1.376	1.195
	0.492	1.387	1.121
9	0.481	1.375	1.144
	0.535	1.192	1.273
11	0.489	1.287	1.224
	0.487	1.400	1.113
13	0.480	1.356	1.164
	0.493	1.394	1.113
14	0.605	1.208	1.187
	0.383	1.288	1.329
15	0.476	1.411	1.113
	0.506	1.416	1.078
17	0.505	1.324	1.171
	0.532	1.202	1.266
19	0.481	1.341	1.178
	0.473	1.343	1.184
21	0.517	1.194	1.289
	0.533	1.223	1.244
23	0.425	1.429	1.146
	0.510	1.278	1.212
25	0.501	1.175	1.324
	0.458	1.241	1.301

**Table 9-4** Punch 4. Cross section zones evolution data

Set	Rollover (mm)	Shear zone height (mm)	Fracture-Burr (mm)
1	1.151	0.505	1.344
	1.131	0.633	1.236
3	1.137	0.518	1.345
	1.159	0.588	1.253
5	1.012	0.583	1.405
	1.118	0.559	1.323
7	1.140	0.522	1.338
	1.147	0.577	1.276
9	1.245	0.637	1.118
	1.145	0.705	1.150
11	1.200	0.677	1.123
	1.224	0.664	1.112
13	1.268	0.611	1.121
	1.180	0.741	1.079
15	1.195	0.665	1.140
	1.204	0.600	1.196
17	1.167	0.548	1.285
	1.098	0.539	1.363
19	1.179	0.556	1.265
	1.169	0.582	1.249
21	1.315	0.796	0.889
	1.259	0.639	1.102
23	1.153	0.679	1.168
	1.176	0.632	1.192
25	1.252	0.650	1.098
	1.247	0.619	1.134